

## A SEARCH FOR “DWARF” SEYFERT NUCLEI. VI. PROPERTIES OF EMISSION-LINE NUCLEI IN NEARBY GALAXIES

LUIS C. HO

The Observatories of the Carnegie Institution of Washington, 813 Santa Barbara St., Pasadena, CA 91101

ALEXEI V. FILIPPENKO

Department of Astronomy, University of California, Berkeley, CA 94720-3411

AND

WALLACE L. W. SARGENT

Palomar Observatory, 105-24 Caltech, Pasadena, CA 91125

*To appear in The Astrophysical Journal.*

## ABSTRACT

We use the database from Paper III to quantify the global and nuclear properties of emission-line nuclei in the Palomar spectroscopic survey of nearby galaxies. We show that the host galaxies of Seyferts, LINERs, and transition objects share remarkably similar large-scale properties and local environments. The distinguishing traits emerge on nuclear scales. Compared with LINERs, Seyfert nuclei are an order of magnitude more luminous and exhibit higher electron densities and internal extinction. We suggest that Seyfert galaxies possess characteristically more gas-rich circumnuclear regions, and hence a more abundant fuel reservoir and plausibly higher accretion rates. The differences between the ionization state of the narrow emission-line regions of Seyferts and LINERs can be partly explained by the differences in their nebular properties. Transition-type objects are consistent with being composite (LINER/H II) systems. With very few exceptions, the stellar population within the central few hundred parsecs of the host galaxies is uniformly old, a finding that presents a serious challenge to starburst or post-starburst models for these objects. Seyferts and LINERs have virtually indistinguishable velocity fields as inferred from their line widths and line asymmetries. Transition nuclei tend to have narrower lines and more ambiguous evidence for line asymmetries. All three classes of objects obey a strong correlation between line width and line luminosity. We argue that the angular momentum content of circumnuclear gas may be an important factor in determining whether a nucleus becomes active. Finally, we discuss some possible complications for the unification model of Seyfert galaxies posed by our observations.

*Subject headings:* galaxies: active — galaxies: nuclei — galaxies: Seyfert — galaxies: starburst — surveys

## 1. INTRODUCTION

Spectroscopic surveys have shown that emission-line nuclei are very common in nearby galaxies (see Ho 1996 and references therein). Particularly striking is the population of galactic nuclei considered “active,” by which we mean objects whose energy source ultimately derives from nonstellar processes associated with accretion onto massive black holes, as is commonly believed to be the case for classical Seyfert nuclei and quasars. According to the survey of Ho, Filippenko, & Sargent (1997b), which is the subject of the papers in this series, 43% of galaxies brighter than  $B_T = 12.5$  mag can be considered active galactic nuclei (AGNs) or AGN candidates. Among these, the majority (2/3) belong to an enigmatic class of sources called low-ionization nuclear emission-line regions (LINERs; Heckman 1980). Ever since their discovery more than 20 years ago, the physical origin of LINERs has been controversial. While it is now generally acknowledged that a significant fraction of LINERs genuinely belong in the AGN family, the situation still remains unclear for the class as a whole. Discussions of the competing models and the evidence for and against them can be found in the reviews by Filippenko (1996), Ho (1999a, 2002), and Barth (2002).

It should be emphasized that settling the physical origin of LINERs is more than of mere phenomenological interest. Because they are so numerous, LINERs could make a tremendous impact on the specification of the faint end of the local AGN luminosity function, which is currently very poorly

known (Huchra & Burg 1992). This, in turn, has ramifications for all astrophysical issues that depend on the statistics of local AGNs or massive black holes.

We completed an extensive optical spectroscopic survey of the central regions of nearly 500 nearby galaxies using the 5-m Hale telescope at Palomar Observatory (Filippenko & Sargent 1985, hereafter Paper I; Ho, Filippenko, & Sargent 1995, 1997a, 1997b, hereafter Papers II, III, and V, respectively; Ho et al. 1997e, hereafter Paper IV; Ho, Filippenko, & Sargent 1997c, 1997d). This is the largest and most sensitive survey of its kind that has resulted in, among other things, the discovery of an unprecedented number of nearby LINERs. This paper systematically examines the statistical properties of the sample of AGN candidates in the Palomar survey. The nature of our survey permits a fresh look at basic properties that can be either directly measured from our spectra or are otherwise available from existing sources. Another objective is to compare the traits of LINERs and a related class of nuclei known as “transition objects” (Ho, Filippenko, & Sargent 1993a; Ho 1996) with those of Seyfert nuclei, in order to test the proposition that most LINERs and LINER-like sources truly are accretion-powered systems. We do not consider H II (star forming) nuclei at length, except insofar as they illuminate the discussion on the AGN candidates; several issues related to H II nuclei were treated in Paper V and Ho et al. (1997c, 1997d).

The quantities analyzed in this paper come from the database in Paper III. Ho (1996) and Filippenko (1996) have given pre-

liminary discussions of some of the results presented here; this paper supersedes the earlier work. As in previous papers in this series, distance-dependent parameters assume a Hubble constant of  $H_0 = 75 \text{ km s}^{-1} \text{ Mpc}^{-1}$ .

## 2. ANALYSIS

The ensuing sections give a comparative analysis of a number of global and nuclear properties of the various subclasses of AGN candidates. We wish to elucidate the fundamental parameters responsible for the observed diversity of spectral characteristics in emission-line nuclei, and ultimately, to gain a better physical understanding of nuclear activity in nearby galaxies. Following the convention established in the earlier papers of this series, we distinguish three categories of AGN-like emission-line nuclei: Seyfert nuclei, LINERs, and “transition objects.” Seyfert nuclei differ from LINERs principally in having higher levels of ionization, and transition objects are characterized by spectra that appear to be intermediate between those of LINERs and nuclear H II regions. In optical line-ratio diagnostic diagrams such as those introduced by Baldwin, Phillips, & Terlevich (1981) and Veilleux & Osterbrock (1987), transition objects populate the region between traditional H II nuclei and LINERs. This prompted Ho et al. (1993a) to suggest that transition objects are composite systems comprised of a normal LINER nucleus whose signal is diluted or contaminated by emission from neighboring regions of recent star formation. If this interpretation is correct, then these sources ought to be included in the overall AGN census, to the extent that LINERs themselves are genuine AGNs. We attempt to test both of these hypotheses — that transition nuclei are closely related to LINERs and that both of these groups are similar to Seyferts. In this paper we adopt the popular viewpoint that all Seyfert nuclei are bona fide AGNs.

Before proceeding further, we make a few remarks on taxonomy. Throughout this paper, for emphasis, we will cast LINERs, transition objects, and Seyferts as distinctly separate groups of emission-line objects. While this approach is useful to highlight general population trends, one should recognize that the classification boundaries are fuzzy. This is obvious from inspection of Figure 7 in Paper III. LINERs and Seyferts do not form a bimodal distribution in ionization; for example, the distribution of the  $[\text{O III}] \lambda 5007/\text{H}\beta$  or  $[\text{O I}] \lambda 6300/[\text{O III}] \lambda 5007$  ratios is continuous for the LINERs and Seyferts in the Palomar survey. In the same vein, the division between LINERs from transition nuclei, or that between transition and H II nuclei, is largely arbitrary. And lastly, contrary to popular misconception, not every weak emission-line nucleus in an early-type galaxy is a LINER. As we will later show, in nearby galaxies LINERs are typically an order of magnitude underluminous compared to Seyferts, but the nuclear luminosities of the two classes overlap generously.

Tables 1a, 2a, and 3a summarize basic statistical properties for the univariate distributions of various global and nuclear parameters. For each parameter, we give the mean, the standard deviation, and the median. Each subclass of object is listed separately. For reasons given in § 2.1, our discussion focuses primarily on the spiral galaxies, and in particular on a subsample restricted to Hubble types Sab–Sbc ( $T = 2–4$ ); however, for completeness, we list also the statistics for the entire sample, ir-

respective of Hubble type. We evaluate censored data sets (containing upper or lower limits) using the Kaplan-Meier product-limit estimator (Feigelson & Nelson 1985). Two-sample comparisons between subclasses (Tables 1b, 2b, and 3b) are performed using the Kolmogorov-Smirnov test, and as a consistency check, also Gehan’s generalized Wilcoxon (hereafter Gehan) test (Isobe, Feigelson, & Nelson 1986). We quote the significance in terms of the probability of rejecting the null hypothesis that the two distributions are drawn from the same parent population,  $P_{\text{null}}$ . We consider two distributions to be statistically different if  $P_{\text{null}} < 5\%$ . The significance of the difference between two means is evaluated using Student’s  $t$  test (Press et al. 1986). For these three tests, we designate the probability of rejecting the null hypothesis as  $P_K$ ,  $P_G$ , and  $P_t$ , respectively.

### 2.1. Host Galaxy Properties

The host galaxies of the AGN candidates show a surprising degree of homogeneity in their large-scale, global properties. We found in Paper V that all three subclasses inhabit galaxies of very similar morphologies, mostly Hubble types ranging from ellipticals to lenticulars and early-type, bulge-dominated spirals (Sbc and earlier). The only noticeable difference is that a larger fraction of elliptical and S0 galaxies contains pure LINERs, and transition objects tend to be found in galaxies of slightly later Hubble type. Table 1a shows that the mean and median morphological index ( $T$ ) of LINERs is about two units earlier than those of transition objects and Seyfert galaxies. When we restrict the comparison to the spiral subsample, the  $T$  distributions for LINERs and Seyferts become quite similar, but transition objects remain statistically different compared to LINERs (Table 1b), by  $\Delta T \approx 1$ . Since many global as well as nuclear properties vary systematically with Hubble type, we must be wary of potential selection effects that can be introduced when comparing samples mismatched in Hubble type. To mitigate this problem, we will concentrate our analysis on a highly restricted subsample comprised only of galaxies with Hubble types Sab–Sbc ( $T = 2–4$ ; hereinafter referred to as “the Sb subsample”)<sup>1</sup>. This range was chosen as a compromise between the desire to isolate a morphologically homogeneous sample for each AGN subclass and the need to retain sufficient numbers for meaningful statistical analysis. With this choice, all three AGN subclasses have a mean and median  $T \approx 3$ . The Sb subsample contains 23 LINERs, 32 transition objects, and 19 Seyferts. For comparison, we also consider a matched subsample of 36 H II nuclei, constructed by combining all the  $T = 2–3$  objects in the parent sample with a randomly chosen subset of  $\sim 1/3$  of the  $T = 4$  objects; we did not use the full sample of H II nuclei with  $T = 4$  hosts because this morphological type contains a higher percentage of H II nuclei than AGNs.

The similarity among the three AGN subclasses can be further discerned in their absolute optical luminosities, which are typically close to, or somewhat in excess of,  $L^*$ . As shown in Table 1b, they also have statistically similar distributions of bulge luminosities [ $M_B(\text{bul})$ ], neutral hydrogen content (H I mass normalized to the optical luminosity,  $M_{\text{HI}}/L_B^0$ ), as well

<sup>1</sup> We are forced to violate this rule when examining issues related to type 1 versus type 2 AGNs, objects with and without detectable broad emission lines, respectively. There would otherwise be insufficient objects for a meaningful analysis. We use, instead, the full subsample of spirals, which fortunately have statistically similar distributions of Hubble types for each of the two types of LINERs and Seyferts (see Table 1b). The subsample of spirals contains 11 LINER 1s, 39 LINER 2s, 18 Seyfert 1s, and 20 Seyfert 2s.

TABLE 1A: STATISTICS OF HOST GALAXY PARAMETERS

Parameter	Class	Number			Mean			$\sigma$			Median		
		All	Spirals	Sb <sup>a</sup>	All	Spirals	Sb <sup>a</sup>	All	Spirals	Sb <sup>a</sup>	All	Spirals	Sb <sup>a</sup>
$T$	L	92	48	23	-0.3	2.4	2.8	3.3	1.9	0.85	0.0	2.0	3.0
	T	65	44	32	1.6	3.4	3.0	3.2	1.8	0.78	2.0	3.0	3.0
	S	51	37	19	1.4	3.0	3.2	3.2	2.0	0.77	2.0	3.0	3.0
	H	206	190	36	4.8	5.0	3.1	2.4	2.1	0.68	5.0	5.0	3.0
$M_{B_T}^0$ (mag)	L	94	50	23	-20.38	-20.51	-20.71	1.02	0.93	0.85	-20.46	-20.50	-20.74
	T	65	44	32	-20.27	-20.29	-20.60	0.97	0.89	0.74	-20.26	-20.32	-20.65
	S	52	38	19	-20.36	-20.55	-20.57	1.31	1.09	0.84	-20.73	-20.84	-20.76
	H	206	190	36	-19.77	-19.77	-20.25	1.67	1.23	0.84	-20.01	-20.03	-20.32
$M_B$ (bul) (mag)	L	92	48	23	-19.41	-18.97	-19.20	1.39	1.37	0.77	-19.46	-19.17	-19.27
	T	65	44	32	-18.80	-18.37	-19.01	1.71	1.71	0.78	-19.15	-18.63	-18.92
	S	51	37	19	-18.89	-18.69	-18.94	1.79	1.81	0.83	-19.23	-19.23	-19.23
	H	188	181	36	-17.28	-17.23	-18.63	1.99	2.01	0.83	-17.85	-17.80	-18.75
$(M_{\text{HI}}/L_B^0)_\odot$	L	94	50	23	0.098	0.13	0.12	0.11	0.13	0.075	0.068	0.10	0.10
	T	64	44	32	0.15	0.20	0.15	0.17	0.18	0.089	0.12	0.16	0.15
	S	50	36	19	0.14	0.17	0.14	0.15	0.16	0.091	0.11	0.12	0.13
	H	206	190	36	0.24	0.25	0.17	0.16	0.16	0.12	0.20	0.22	0.17
$D_{25}$ (kpc)	L	94	50	23	29.9	31.2	33.9	15.3	15.5	16.9	26.4	26.5	28.4
	T	65	44	32	27.6	29.2	31.7	12.1	12.5	12.8	26.7	27.5	27.8
	S	52	38	19	29.1	30.9	30.1	13.1	12.1	10.7	27.9	30.7	29.7
	H	206	190	36	23.9	22.7	25.2	22.1	11.3	12.0	21.9	22.1	22.9
$d$ (Mpc)	L	94	50	23	26.2	25.4	26.3	16.2	15.9	15.3	22.2	21.4	26.1
	T	65	44	32	22.3	20.5	21.6	13.0	11.9	12.7	17.0	17.0	17.0
	S	52	38	19	26.5	25.7	19.1	17.8	17.2	11.6	20.4	20.4	16.8
	H	206	190	36	21.1	20.4	25.0	14.4	12.8	13.5	17.1	17.0	22.3
$i$ (degrees)	L	72	50	23	49.3	48.9	47.7	18.4	18.0	19.1	50.0	49.0	43.0
	T	55	40	28	55.9	56.7	56.3	16.1	16.5	16.3	58.0	58.0	57.5
	S	44	35	18	46.8	48.2	51.7	16.7	17.1	16.6	44.5	46.0	50.5
	H	190	175	32	52.1	51.9	54.5	18.4	18.0	15.3	53.5	53.0	56.0
$(U - B)_T^0$ (mag)	L	74	36	17	0.36	0.22	0.17	0.17	0.14	0.13	0.38	0.25	0.19
	T	51	31	22	0.24	0.098	0.12	0.23	0.17	0.12	0.23	0.11	0.11
	S	35	22	9	0.22	0.12	0.064	0.23	0.20	0.17	0.25	0.065	0.020
	H	126	114	24	-0.057	-0.079	0.031	0.18	0.16	0.15	-0.095	-0.10	0.030
$(B - V)_T^0$ (mag)	L	85	44	20	0.82	0.73	0.69	0.13	0.12	0.12	0.84	0.76	0.72
	T	59	38	27	0.74	0.65	0.66	0.15	0.11	0.078	0.74	0.67	0.67
	S	47	34	17	0.72	0.66	0.64	0.15	0.13	0.11	0.74	0.66	0.62
	H	168	156	28	0.54	0.52	0.60	0.15	0.14	0.12	0.52	0.52	0.59
$L_{\text{FIR}}/L_B^0$	L	83	46	22	0.078	0.12	0.12	0.081	0.084	0.091	0.054	0.094	0.091
	T	62	42	31	0.19	0.27	0.21	0.34	0.39	0.16	0.099	0.17	0.17
	S	50	38	19	0.21	0.25	0.25	0.23	0.24	0.26	0.12	0.18	0.13
	H	198	182	34	0.36	0.34	0.51	0.55	0.49	0.49	0.23	0.23	0.41
$S_{60}/S_{100}$	L	75	46	22	0.42	0.33	0.28	0.41	0.13	0.099	0.33	0.31	0.26
	T	59	42	31	0.34	0.32	0.30	0.12	0.12	0.099	0.34	0.32	0.31
	S	48	38	19	0.40	0.41	0.38	0.18	0.15	0.16	0.36	0.38	0.35
	H	197	181	34	0.41	0.40	0.43	0.13	0.13	0.13	0.40	0.39	0.42
$S_{25}/S_{60}$	L	72	45	21	0.26	0.14	0.11 <sup>b</sup>	0.31	0.077	0.014 <sup>b</sup>	0.16	0.12	0.095 <sup>b</sup>
	T	59	42	31	0.16	0.14	0.12 <sup>b</sup>	0.13	0.084	0.008 <sup>b</sup>	0.13	0.13	0.12 <sup>b</sup>
	S	47	38	19	0.27	0.25	0.20 <sup>b</sup>	0.23	0.22	0.043 <sup>b</sup>	0.16	0.16	0.13 <sup>b</sup>
	H	198	182	34	0.14	0.13	0.13	0.086	0.084	0.050	0.12	0.12	0.13
$\rho_{\text{gal}}$ (Mpc <sup>-3</sup> )	L	82	45	20	0.78	0.64	0.63	0.89	0.74	0.75	0.44	0.30	0.36
	T	57	40	28	0.89	0.65	0.64	1.04	0.67	0.70	0.39	0.34	0.34
	S	43	32	18	0.83	0.75	1.07	1.04	0.92	1.13	0.38	0.38	0.53
	H	184	172	29	0.63	0.60	0.72	0.75	0.72	0.79	0.30	0.30	0.44
$\theta_p$ ( $D_{25}$ )	L	94	50	23	17.9	20.2	18.7 <sup>b</sup>	21.5	20.3	3.9 <sup>b</sup>	9.3	13.9	10.5 <sup>b</sup>
	T	65	44	32	20.3	19.3	23.1 <sup>b</sup>	24.2	19.1	4.4 <sup>b</sup>	13.6	13.1	14.9 <sup>b</sup>
	S	52	38	19	21.9	20.9	17.0 <sup>b</sup>	21.2	20.1	4.5 <sup>b</sup>	12.7	12.7	8.9 <sup>b</sup>
	H	202	187	36	27.4	28.3	40.9 <sup>b</sup>	28.9	29.6	8.5 <sup>b</sup>	18.8	20.0	15.4 <sup>b</sup>

<sup>a</sup>Hubble types Sab–Sbc ( $T = 2 - 4$ ).

<sup>b</sup>Calculated using the Kaplan-Meier product-limit estimator (Feigelson & Nelson 1985).

TABLE 1B: COMPARISON OF HOST GALAXY PARAMETERS

Parameter	Test	L/T	L/S	L1/L2	S1/S2	L+T+S/H
$T$	$P_K$	0.319	0.614	0.346	0.987	0.623
	$P_G$	0.285	0.157	0.184	0.975	0.357
	$P_t$	0.299	0.154	0.0936	0.779	0.316
$M_{BT}^0$	$P_K$	0.541	0.464	0.957	0.680	0.0736
	$P_G$	0.631	0.716	0.543	0.447	0.0375
	$P_t$	0.618	0.602	0.660	0.556	0.0284
$M_B$ (bul)	$P_K$	0.756	0.419	0.309	0.899	0.0827
	$P_G$	0.386	0.408	0.264	0.522	0.0222
	$P_t$	0.374	0.297	0.124	0.469	0.0136
$(M_{\text{HI}}/L_B^0)_\odot$	$P_K$	0.437	0.666	0.703	0.332	0.131
	$P_G$	0.139	0.606	0.654	0.428	0.116
	$P_t$	0.109	0.414	0.812	0.655	0.0986
$D_{25}$	$P_K$	0.618	0.419	0.346	0.916	0.0131
	$P_G$	0.891	0.752	0.461	0.704	$5.6 \times 10^{-3}$
	$P_t$	0.602	0.382	0.525	0.828	$9.9 \times 10^{-3}$
$d$	$P_K$	0.235	0.0972	0.478	0.228	0.609
	$P_G$	0.312	0.144	0.512	0.225	0.249
	$P_t$	0.231	0.0919	0.217	0.524	0.344
$i$	$P_K$	0.207	0.825	0.738	0.997	0.444
	$P_G$	0.0830	0.450	0.574	0.667	0.619
	$P_t$	0.0972	0.476	0.549	0.641	0.710
$(U - B)_T^0$	$P_K$	0.309	0.0794	0.458	0.147	0.0437
	$P_G$	0.151	0.0603	0.309	0.324	0.0136
	$P_t$	0.176	0.115	0.111	0.225	0.0123
$(B - V)_T^0$	$P_K$	0.0709	0.107	0.753	0.673	0.0227
	$P_G$	0.0823	0.168	0.953	0.358	$5.8 \times 10^{-3}$
	$P_t$	0.327	0.212	0.949	0.269	0.0159
$L_{\text{FIR}}/L_B^0$	$P_K$	0.0366	0.0749	0.817	0.325	$1.4 \times 10^{-5}$
	$P_G$	0.0195	0.0666	0.579	0.953	$< 1 \times 10^{-5}$
	$P_t$	0.0151	0.0478	0.409	0.782	$7.1 \times 10^{-4}$
$S_{60}/S_{100}$	$P_K$	0.239	0.0344	0.621	0.0583	$1.0 \times 10^{-3}$
	$P_G$	0.307	0.0123	0.515	0.0923	$1.0 \times 10^{-4}$
	$P_t$	0.425	0.0256	0.739	0.0418	$5.9 \times 10^{-5}$
$S_{25}/S_{60}$	$P_K^a$	...	...	...	...	...
	$P_G$	0.356	0.0199	0.124	0.0278	0.355
	$P_t^a$	...	...	...	...	...
$\rho_{\text{gal}}$	$P_K$	0.937	0.395	0.364	0.0159	0.987
	$P_G$	0.754	0.149	0.212	0.0110	0.885
	$P_t$	0.935	0.174	0.301	0.177	0.871
$\theta_p$	$P_K$	0.919	0.666	0.346	0.0135	0.204
	$P_G$	0.777	0.560	0.482	0.0030	0.116
	$P_t$	0.577	0.848	0.605	0.0053	0.0378

NOTE.—The two-sample tests are restricted to the subsample of Sab–Sbc galaxies, with the exception of the comparisons between type 1 and type 2 objects (L1/L2 and S1/S2), which use the entire sample of spirals.  $P_K$  and  $P_G$  are the probabilities for rejecting the hypothesis that two samples are drawn from the same parent population according to the Kolmogorov-Smirnov test and the Gehan’s generalized Wilcoxon test (Isobe, Feigelson, & Nelson 1986), respectively. Student’s  $t$  test ( $P_t$ ) evaluates the null hypothesis that two samples have the same mean. The subclasses of emission-line objects follow the notation of Paper III, where H = H II nucleus, L = LINER, T = transition object (LINER/H II nucleus), S = Seyfert, and “1” and “2” denote type 1 and type 2 nuclei, respectively.

<sup>a</sup>Statistic not calculated because of the large number of censored data points.

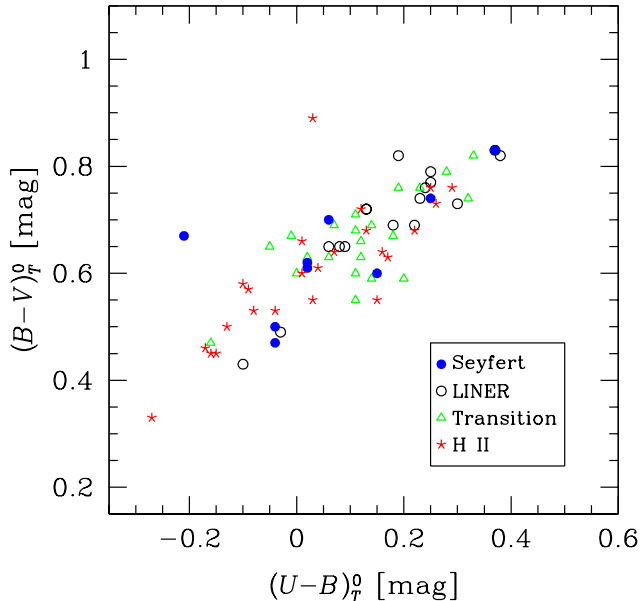


FIG. 1.— Optical colors of Seyferts (solid circles), LINERs (open circles), transition objects (triangles), and H II nuclei (stars). The colors are based on integrated magnitudes corrected to face-on orientation. Only Sab–Sbc galaxies are shown.

as optical isophotal diameters ( $D_{25}$ ). Transition objects may be marginally more highly inclined than LINERs, although the statistical significance is low ( $P_K = 21\%$ ,  $P_G = 8.3\%$ , and  $P_t = 9.7\%$ ), whereas LINERs are indistinguishable from Seyfert galaxies; we will revisit this point in § 3.3.

The most interesting differences emerge from inspection of the broad-band, integrated optical colors (Fig. 1) and the far-infrared (FIR) properties (Fig. 2). Two patterns deserve attention. Relative to LINERs, transition objects exhibit enhanced FIR emission (for a given optical luminosity), at the level of  $P_{\text{null}} \approx 1\%–4\%$ . There are no obvious differences in their FIR colors. This might reflect an elevated level of star formation, either global or nuclear, in transition objects. Consistent with this hypothesis, transition objects show mildly bluer integrated  $U–B$  and  $B–V$  colors, although the level of significance is low. Interestingly, Seyfert galaxies too tend to have higher normalized FIR luminosities and somewhat bluer optical colors compared to LINERs. But these two groups also occupy slightly different loci in the FIR color-color diagram (Fig. 2a): Seyferts have statistically “hotter” FIR colors (higher  $S_{60}/S_{100}$  and  $S_{25}/S_{60}$  flux density ratios). Although one might also attribute these characteristics to enhanced star formation in the Seyfert population, we note that the  $S_{25}/S_{60}$  ratios of the Seyferts are generally larger than those in H II nuclei. This suggests that the enhanced FIR emission and hotter FIR colors in Seyferts may instead be due to a higher level of AGN activity in these objects.

We note that the two types of Seyfert galaxies in our sample differ in their FIR properties: Seyfert 1s possess higher  $S_{60}/S_{100}$  and  $S_{25}/S_{60}$  ratios than Seyfert 2s. We will discuss the implications of this result in § 3.5. The two Seyfert types show no other obvious differences in global properties. LINER 1s and LINER 2s cannot be distinguished on the basis of their global properties.

## 2.2. Environment

Tidal interaction with neighboring galaxies is often cited as a possible mechanism for triggering nuclear activity. Paper III gives two parameters that can be used to evaluate the importance of this effect in our sample: (1)  $\rho_{\text{gal}}$ , defined by Tully (1988) as the density of all galaxies brighter than  $M_B = -16$  mag in the object’s local vicinity, and (2)  $\theta_p$ , the projected angular separation to the nearest neighbor within a magnitude difference of  $\pm 1.5$  mag and a velocity difference of  $\pm 500$  km s $^{-1}$ , measured in units of the isophotal angular diameter of the primary galaxy,  $D_{25}$ . After excluding the elliptical and S0 galaxies, whose overrepresentation among LINERs might bias that sample because of the morphology-density relation (Dressler 1980; Postman & Geller 1984), we find that the local environment, as measured by  $\rho_{\text{gal}}$  and  $\theta_p$ , has no impact on the spectral classification of the nucleus. The same conclusion holds for the Sb subsample.

The only exception concerns the two subtypes of Seyfert galaxies: to a relatively high level of significance, Seyfert 1s inhabit denser environments than Seyfert 2s. The mean and median galaxy density for Seyfert 1s is 1 and 0.6 Mpc $^{-3}$ , compared with 0.5 and 0.3 Mpc $^{-3}$  for Seyfert 2s. Even more striking is the projected distance to the nearest neighbor. For Seyfert 1s, the mean and median value of  $\theta_p$  is  $\sim 12$  and 7  $D_{25}$ ; for Seyfert 2s, the corresponding values are  $\theta_p \approx 29$  and 23  $D_{25}$ . In terms of  $\theta_p$ , the differences between the two samples are significant at the level of  $P_K = 1.3\%$ ,  $P_G = 0.3\%$ , and  $P_t = 0.5\%$ .

## 2.3. Nuclear Properties

We consider several nebular parameters that might provide clues to the physical conditions of the line-emitting regions (see Tables 2a and 2b). We find no significant differences between LINERs and transition objects in terms of line luminosity $^2$  ( $L_{\text{H}\alpha}$ ; Fig. 3), line equivalent width [EW( $\text{H}\alpha$ )], or electron density ( $n_e$ ; Fig. 4). An interesting trend seen in the sample of transition objects, but absent from the others, is the tendency for more highly inclined sources to show larger amounts of internal reddening (Fig. 5). The Kendall’s  $\tau$  correlation coefficient between  $E(B–V)_{\text{int}}$  and  $i$  is  $r = 0.70$ , significant at the level of 99%. The source of dust opacity in transition objects evidently is somehow coupled to the large-scale disk component of the galaxy. On average, transition objects tend to be marginally more reddened than LINERs [ $\langle E(B–V)_{\text{int}} \rangle = 0.36$  vs. 0.19 mag;  $P_t = 4.0\%$ ]; the reddening distributions for the two classes may be inconsistent with being drawn from the same parent population ( $P_K = 3.6\%$  and  $P_G = 9.7\%$ ; Fig. 6).

By contrast, LINERs stand out from Seyfert nuclei in several important respects. LINERs have weaker emission lines [ $\langle \text{EW}(\text{H}\alpha) \rangle$  smaller by a factor of  $\sim 8$ ], lower  $\text{H}\alpha$  luminosity (factor of  $\sim 11$  in  $\langle L_{\text{H}\alpha} \rangle$ ), lower density (factor of  $\sim 3$  in  $\langle n_e \rangle$ ), and lower internal reddening [factor of  $\sim 2$  in  $\langle E(B–V)_{\text{int}} \rangle$ ]. The differences between the two samples for all these parameters are highly significant according to the Kolmogorov-Smirnov, Gehan, and Student’s  $t$  tests when the full sample of spirals is considered. The statistical significances are somewhat diminished for the Sb subsample, probably because of the more limited statistics. Nevertheless, even a visual inspection of Figures 3, 4, and 6 leaves little doubt that LINERs and Seyferts have systematically different nebular properties. As discussed

<sup>2</sup> Some of the objects in the Palomar survey were observed under nonphotometric conditions. Whenever possible, we supplemented the database in Paper III with  $\text{H}\alpha$  luminosities published in the literature. A list of these data is given in the Appendix.

TABLE 2A: STATISTICS OF NEBULAR PARAMETERS

Parameter	Class	Number			Mean			$\sigma$			Median		
		All	Spirals	Sb <sup>a</sup>	All	Spirals	Sb <sup>a</sup>	All	Spirals	Sb <sup>a</sup>	All	Spirals	Sb <sup>a</sup>
EW(H $\alpha$ ) ( $\text{\AA}$ )	L	93	50	23	3.1	3.5	3.9	4.1	4.6	5.9	1.9	2.2	2.2
	T	64	44	32	3.1	3.8	3.0	4.2	4.8	2.5	1.7	2.0	2.0
	S	52	38	19	18	23	30	45	51	66	3.5	4.6	3.3
	H	204	187	35	63	63	19	183	190	18	18	18	12
$L_{\text{H}\alpha}$ ( $10^{38}$ erg s <sup>-1</sup> )	L	83	42	21	30.6	39.0	24.3	57.8	67.7	51.1	6.6	8.1	8.1
	T	59	40	29	33.7	41.8	30.0	85.7	102	62.5	7.4	7.3	8.1
	S	51	37	19	288	320	271	664	718	782	37.2	51.3	27.5
	H	187	171	33	193	165	270	561	477	476	18.2	15.9	79.4
$n_e$ (cm <sup>-3</sup> )	L	83	46	22	281	272	213	275	291	168	210	198	193
	T	63	44	32	264	244	235	325	318	278	176	150	177
	S	50	38	19	469	499	559	291	294	309	409	473	482
	H	204	187	36	184	175	234	204	194	177	120	106	222
$E(B - V)_{\text{int}}$ (mag)	L	90	50	23	0.18	0.22	0.19	0.26	0.29	0.25	0.035	0.075	0.080
	T	60	41	31	0.34	0.37	0.36	0.41	0.43	0.37	0.22	0.35	0.37
	S	50	37	18	0.43	0.44	0.40	0.49	0.46	0.38	0.33	0.36	0.42
	H	203	188	35	0.47	0.46	0.65	0.35	0.34	0.38	0.43	0.41	0.58
FWHM([N II]) (km s <sup>-1</sup> )	L	90	48	22	339	304	294	144	130	127	341	287	268
	T	62	43	32	253	209	221	125	78	79	221	198	215
	S	51	38	19	303	309	279	166	179	174	273	263	227
	H	203	187	36	135	133	164	61	58	60	123	124	170

<sup>a</sup>Hubble types Sab–Sbc ( $T = 2 - 4$ ).

TABLE 2B: COMPARISON OF NEBULAR PARAMETERS

Parameter	Test	L/T	L/S	L1/L2	S1/S2	L+T+S/H
EW(H $\alpha$ )	$P_K$	0.975	0.167	0.0809	0.154	$<1 \times 10^{-5}$
	$P_G$	0.885	0.0513	0.0382	0.0273	$<1 \times 10^{-5}$
	$P_t$	0.497	0.109	0.429	0.0590	0.0782
$L_{\text{H}\alpha}$	$P_K$	0.917	0.0936	0.124	0.446	$5.7 \times 10^{-4}$
	$P_G$	0.868	0.100	0.159	0.544	$2.0 \times 10^{-4}$
	$P_t$	0.828	0.0607	0.522	0.206	$5.3 \times 10^{-5}$
$n_e$	$P_K$	0.837	$1.7 \times 10^{-4}$	0.459	0.0321	0.417
	$P_G$	0.766	$<1 \times 10^{-5}$	0.205	0.0114	0.353
	$P_t$	0.715	$1.7 \times 10^{-4}$	0.267	0.0078	0.0862
$E(B - V)_{\text{int}}$	$P_K$	0.0361	0.0452	0.535	0.489	$3.1 \times 10^{-4}$
	$P_G$	0.0971	0.0271	0.818	0.156	$<1 \times 10^{-5}$
	$P_t$	0.0403	0.0475	0.477	0.158	$5.9 \times 10^{-5}$
FWHM([N II])	$P_K$	0.108	0.517	0.0691	0.264	$3.3 \times 10^{-5}$
	$P_G$	0.0309	0.275	0.0290	0.121	$<1 \times 10^{-5}$
	$P_t$	0.0215	0.747	0.0369	0.257	$<1 \times 10^{-5}$

NOTE.—The two-sample tests are restricted to the subsample of Sab–Sbc galaxies, with the exception of the comparisons between type 1 and type 2 objects (L1/L2 and S1/S2), which use the entire sample of spirals.  $P_K$  and  $P_G$  are the probabilities for rejecting the hypothesis that two samples are drawn from the same parent population according to the Kolmogorov-Smirnov and Gehan’s generalized Wilcoxon tests, respectively. Student’s  $t$  test ( $P_t$ ) evaluates the null hypothesis that two samples have the same mean. The subclasses of emission-line objects follow the notation of Paper III, where H = H II nucleus, L = LINER, T = transition object (LINER/H II nucleus), S = Seyfert, and “1” and “2” denote type 1 and type 2 nuclei, respectively.

in more detail in § 3.2, these trends strongly suggest that the host galaxies of LINERs, and in particular their circumnuclear regions, contain less gaseous material than the host galaxies of Seyfert nuclei. We will argue that this difference may translate into a difference in the amount of fuel available to power the nuclei.

We note that the electron densities given here, which were derived from the ratio of the [S II]  $\lambda\lambda 6716, 6731$  lines using the code of Shaw & Dufour (1993) and the S<sup>+</sup> atomic data of Cai & Pradhan (1993), are significantly lower than the values typically

quoted in older studies of LINERs (e.g., Stauffer 1982b; Keel 1983c; Phillips et al. 1986) and Seyferts (e.g., Koski 1978). Most of the differences can be attributed to revisions in the atomic data.

#### 2.4. Kinematic Properties of the Nuclear Gas

The kinematic information contained in the profiles of the emission lines provides additional constraints on the physical conditions of the circumnuclear environment. Previous

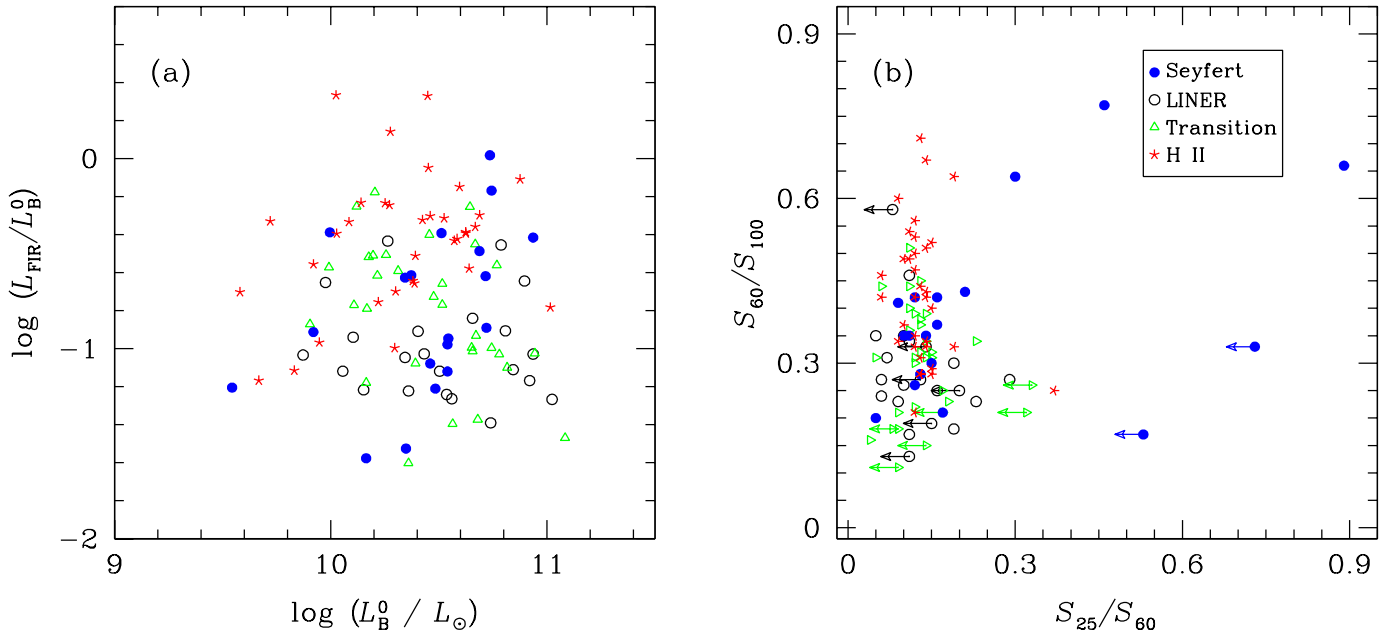


FIG. 2.— FIR properties of Seyferts (solid circles), LINERs (open circles), transition objects (triangles), and H II nuclei (stars) derived from *IRAS* data. Only Sab–Sbc galaxies are shown. Panel (a) plots the FIR luminosity,  $L_{\text{FIR}}$ , normalized to the inclination-corrected  $B$ -band luminosity,  $L_B^0$ , versus  $L_B^0$ . Panel (b) plots the FIR colors  $S_{60}/S_{100}$  versus  $S_{25}/S_{60}$ . Note that Seyferts have systematically stronger FIR emission and hotter FIR colors than LINERs.

kinematic studies have concentrated almost exclusively on Seyferts. Aside from a small handful of relatively crude line width measurements (e.g., Dahari & De Robertis 1988; Whittle 1993, and references therein), little else is known about the line profiles of LINERs as a class. Scarcer still are data for transition objects. Indeed, with a few exceptions, the full width at half maximum (FWHM) of the forbidden lines in LINERs

rarely exceeds  $500 \text{ km s}^{-1}$ , the typical resolution of many previous surveys. Since the initial study of Heckman (1980), it has commonly been assumed that the line widths of LINERs are roughly comparable to those of Seyferts (Wilson & Heckman 1985; Whittle 1985b, 1993), although Stauffer (1982b) has remarked, admittedly based on very small number statistics, that

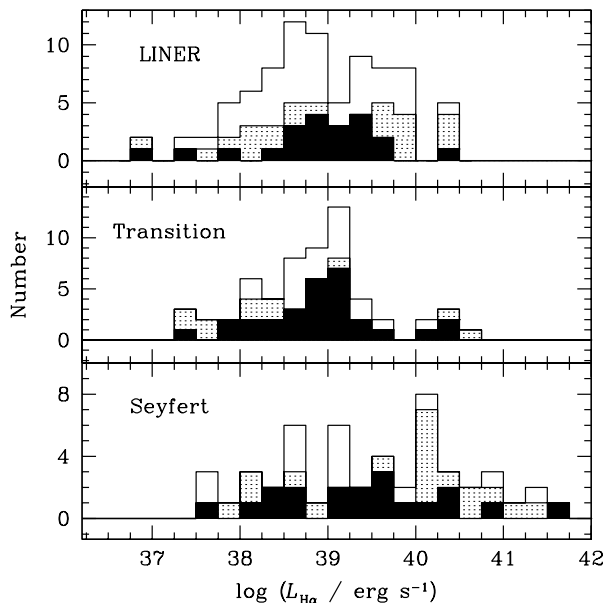


FIG. 3.— Distribution of extinction-corrected luminosities of the narrow  $H\alpha$  emission line for the different classes of AGNs. The bins are separated by 0.25 in logarithmic units. The open histograms plot the E and S0 galaxies, the shaded histograms plot the spiral galaxies excluding Sab–Sbc, and the solid histograms plot the Sab–Sbc galaxies.

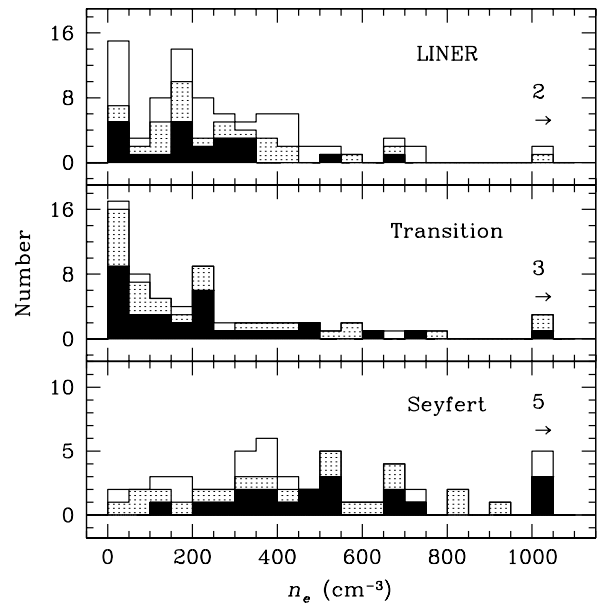


FIG. 4.— Distribution of electron densities, derived from  $[S \text{ II}] \lambda\lambda 6716, 6731$ , for the different classes of AGNs. The bins are separated by units of  $50 \text{ cm}^{-3}$ . The last bin contains all objects with  $n_e > 1000 \text{ cm}^{-3}$ , and the number of such objects is indicated. The open histograms plot the E and S0 galaxies, the shaded histograms plot the spiral galaxies excluding Sab–Sbc, and the solid histograms plot the Sab–Sbc galaxies.

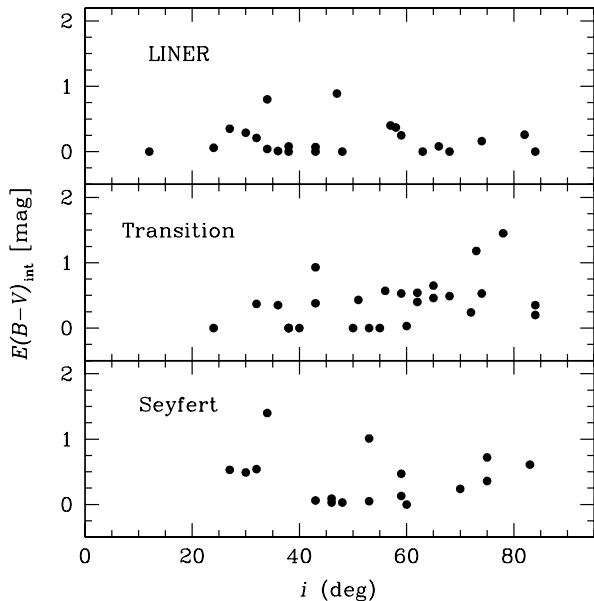


FIG. 5.— Internal reddening of the line-emitting regions plotted against the inclination angle of the host galaxies. The inclination angles, tabulated in Paper III, are derived from the isophotal axial ratios. A slight trend toward larger reddening values in high-inclination (edge-on) systems may be present in transition objects, while no correlation is apparent for LINERs and Seyferts. Only Sab–Sbc galaxies are shown.

LINERs seem to have broader lines than Seyferts. The study of Phillips et al. (1986), whose spectral resolution is comparable to that of the Palomar survey, also has clearly shown that the typical line widths in LINERs are substantially smaller than what Heckman had first thought.

Two simple kinematic parameters can be extracted from the narrow emission lines: their width and sense of asymmetry. As explained in Paper III, in the Palomar survey the line of choice for profile measurement is  $[\text{N II}] \lambda 6583$ , whose width is represented by its FWHM.

#### 2.4.1. Line Widths

The line widths range from being nearly unresolved ( $\sim 100 \text{ km s}^{-1}$ ) to  $500\text{--}700 \text{ km s}^{-1}$ , with an average FWHM of 339, 253, and  $303 \text{ km s}^{-1}$ , respectively, for the entire sample of LINERs, transition objects, and Seyferts (Fig. 7). After isolating the Sb subsample, the values become 294, 221, and  $279 \text{ km s}^{-1}$ , respectively. Transition objects tend to have narrower lines than LINERs, with marginal significance ( $P_K = 11\%$ ,  $P_G = 3.1\%$ , and  $P_I = 2.2\%$ ). LINERs and Seyferts, on the other hand, are virtually identical in terms of their line widths.

In the central regions of galactic bulges, the velocity dispersion of the ionized gas generally traces the velocity dispersion of the stars (Bertola et al. 1984; Whittle 1992; Nelson & Whittle 1996). Thus, at first sight, the narrower lines seen in transition objects appear to indicate that the bulges of their host galaxies have systematically shallower gravitational potential wells. This interpretation, however, conflicts with our knowledge of the host galaxies (§ 2.1) — the morphological types, absolute magnitudes, and especially the bulge luminosities are very similar among the three AGN subclasses. We suggest another explanation: the ionized gas in transition objects is kinematically colder than in LINERs or Seyferts. This may arise, for example, if the line-emitting clouds preferentially lie in a rotationally supported disk.

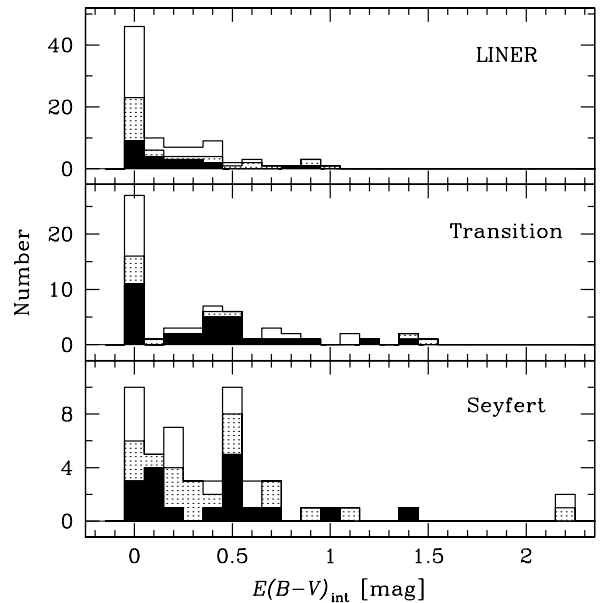


FIG. 6.— Distribution of internal reddening values, inferred from comparison of the observed  $\text{H}\alpha/\text{H}\beta$  ratios to the theoretical value of 3.1 (Halpern & Steiner 1983) and assuming the Galactic extinction curve of Cardelli, Clayton, & Mathis (1989). The bins are separated by units of 0.1 mag. The open histograms plot the E and S0 galaxies, the shaded histograms plot the spiral galaxies excluding Sab–Sbc, and the solid histograms plot the Sab–Sbc galaxies.

As first noticed by Phillips, Charles, & Baldwin (1983), and later quantified more extensively by Whittle (1985b, 1992), the luminosities of the forbidden lines in Seyfert nuclei positively correlate with their widths. The interpretation of this correlation has been controversial, however, mainly because of the existence of other mutual dependences between line width, line luminosity, and radio power (Wilson & Heckman 1985). Whittle (1992) suggests that the fundamental parameter driving all these correlations is the bulge mass (or central gravitational potential) of the host galaxy. The Seyferts in our sample also display a strong correlation between line luminosity and line width (Fig. 8), extending it down in luminosity by over two orders of magnitude compared to previously published samples. For the  $[\text{O III}] \lambda 5007$  line, Whittle (1985b) reported a very steep relation with a slope of  $\sim 6.4$ . We fitted our data using an unweighted linear regression line, calculated using the ordinary least-squares solution bisector with jackknife resampling (Feigelson & Babu 1992), of the form  $\log L_{\text{H}\alpha} = a \log \text{FWHM}([\text{N II}]) + b$ . We find  $(a, b) = (4.7 \pm 0.6, 28.2 \pm 1.4)$  for the spiral subsample and  $(a, b) = (5.7 \pm 0.9, 25.6 \pm 2.3)$  for the entire sample. Figure 8 shows — to our knowledge for the first time — that LINERs also obey the line luminosity-width correlation; Wilson & Heckman (1985) previously concluded that they do not. Interestingly, the slope of the correlation in LINERs is noticeably shallower than in Seyferts; the fits for the spiral and entire sample yield, respectively,  $(a, b) = (3.2 \pm 0.8, 31.3 \pm 2.0)$  and  $(2.7 \pm 0.5, 32.3 \pm 1.3)$ . Transition objects behave essentially the same as the LINERs:  $(a, b) = (3.5 \pm 0.5, 30.7 \pm 1.2)$  for the spirals and  $(a, b) = (2.9 \pm 0.6, 32.0 \pm 1.4)$  for the entire sample. Finally, combining all three AGN subtypes, we obtain  $(a, b) = (4.0 \pm 0.3, 29.5 \pm 0.8)$  and  $(3.6 \pm 0.4, 30.4 \pm 1.0)$  for the spiral and entire sample, respectively. (We confirmed that the Sb subsample gives very similar fits as the full spiral sample.)

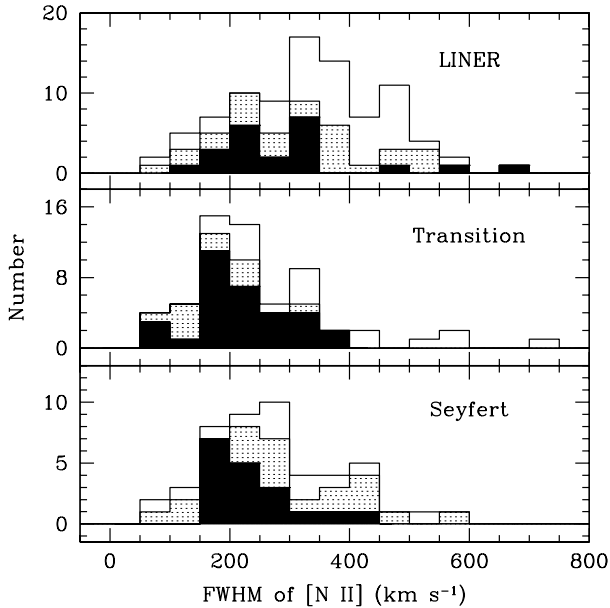


FIG. 7.— Distribution of line widths (FWHM) of the  $[\text{N II}] \lambda 6583$  line for the different classes of AGNs. The line widths have been corrected for instrumental resolution. The bins are separated by units of  $50 \text{ km s}^{-1}$ . The open histograms plot the E and S0 galaxies, the shaded histograms plot the spiral galaxies excluding Sab–Sbc, and the solid histograms plot the Sab–Sbc galaxies.

Keel (1983c) found that in his sample the widths of the forbidden lines are well correlated with galaxy inclination angle, which suggests that motion in the plane of the galaxy disk dominates the velocity field of the narrow-line region (NLR). The present data set does not support this conclusion; no dependence between  $\text{FWHM}([\text{N II}])$  and galaxy inclination angle is seen for the AGN subclasses, either individually or combined. Other studies have come to a similar conclusion (Heckman et al. 1981; Wilson & Heckman 1985; Whittle 1985b; Véron & Véron-Cetty 1986). One can infer that either the NLR does not have a disklike geometry in the plane of the galactic disk, or that the component of the velocity field in the galactic plane contributes only a portion of the total observed line widths (Whittle 1985b, 1992).

We mention, in passing, that in light of the dependence of line width on luminosity, it is hardly surprising that the typical Seyfert nucleus has much narrower lines than conventionally assumed. Hence, the criterion for distinguishing Seyfert 2 nuclei from “normal” emission-line nuclei (i.e., H II nuclei) based on the widths of the narrow lines, either as originally proposed by Weedman (1970, 1977), or as later modified by Balzano & Weedman (1981), Shuder & Osterbrock (1981), and Feldman et al. (1982) is clearly inappropriate for the majority of the Seyfert galaxy population and should be abandoned.

#### 2.4.2. Line Asymmetry

Of course, the FWHM is the crudest, first-order characterization of the line profile. Actually, the shapes of the emission lines in most emission-line nuclei, when examined with sufficient spectral resolution (e.g., Heckman et al. 1981; Whittle 1985a; Veilleux 1991; Paper IV), deviate far from simple symmetric functions (such as a Gaussian), often exhibiting weak extended wings and asymmetry. In fact, most Seyfert nuclei have asymmetric narrow lines, and there seems to be a preponderance of blue wings, usually interpreted as evidence of a substantial radial component in the velocity field coupled with a

source of dust opacity. It would be highly instructive to see if this trend extends to LINERs and transition objects, as it could offer insights into possible differences between the NLRs of objects with high and low ionization.

The majority of the objects in our survey have emission-line spectra of adequate signal-to-noise ratio (S/N) that possible profile asymmetries can be discerned (see Fig. 9 in Ho 1996 and additional examples in Paper IV). Since the red spectra of our survey have higher dispersion than the blue spectra (FWHM resolution  $\sim 100 \text{ km s}^{-1}$  vs.  $225 \text{ km s}^{-1}$ ; see Paper III), we will work with the red spectra. While formalisms have been developed to quantify line asymmetries (e.g., Whittle 1985a), here we take a simpler approach. All the red spectra were visually examined and assigned an “asymmetry code” according to the profile shape of the  $\text{H}\alpha$ ,  $[\text{N II}]$ , and  $[\text{S II}]$  lines: “B” (blue), “R” (red), and “S” (symmetric). Ambiguous cases, or those with low S/N, were excluded. At the resolution of the Palomar survey, and for the typical velocity dispersions of our galaxies, the individual components of the  $\text{H}\alpha + [\text{N II}]$  complex and the  $[\text{S II}]$  doublet have well-separated peaks. For objects with adequate S/N, the sense of the asymmetry is generally noticeable on the profile at 80% of the peak intensity, or less.

The majority of Seyferts ( $\gtrsim 90\%$ ) have sufficient S/N to be classified. The results are as follows: 29% S, 46% B, and 25% R. These percentages remain essentially unchanged for the spiral subsample (31% S, 50% B, and 19% R). Quite remarkably, LINERs show virtually identical statistics. For the objects that are classifiable ( $\sim 75\%$ ), we find 30% S, 46% B, and 24% R (all Hubble types) and 26% S, 58% B, and 16% R (spirals only). Blue asymmetric profiles are preferentially seen in both types of objects. Transition objects seem to depart from this trend. Among the 75% of the sample that can be studied, most show symmetric profiles and there is no obvious preference for blue or red asymmetry (all Hubble types: 52% S, 25% B, and 23% R; spirals only: 56% S, 26% B, and 18% R). We consider the results for transition objects somewhat less certain because their narrower lines (§ 2.4.1) make it more difficult to notice profile asymmetries. Moreover, if a significant portion of the line core in transition objects comes from H II regions, asymmetries from the AGN component, if present, would be most readily detectable in the wings of the profile, which are much more dependent on S/N. (Again, there are no gross differences between the Sb subsample and the full spiral sample.)

To summarize: LINERs and Seyferts exhibit similar trends in their narrow-line asymmetries, and when present, the sense of the asymmetry is preferentially to the blue.

#### 2.4.3. Comparison of Profiles for Different Lines

Detailed studies of Seyferts (e.g., De Robertis & Osterbrock 1984, 1986) and LINERs (Filippenko & Halpern 1984; Filippenko 1985; Filippenko & Sargent 1988; Ho et al. 1993a, 1996; Barth et al. 2001) have found that the widths of the forbidden lines correlate positively with their critical densities. This empirical trend has been interpreted as evidence that the NLRs of these objects contain a wide range of gas densities ( $10^2$ – $10^7 \text{ cm}^{-3}$ ), stratified such that the denser material is located closer to the center. In such a picture,  $[\text{O I}] \lambda 6300$  ( $n_{\text{crit}} \approx 10^6 \text{ cm}^{-3}$ ) should be broader than  $[\text{S II}] \lambda \lambda 6716, 6731$  ( $n_{\text{crit}} \approx 3 \times 10^3 \text{ cm}^{-3}$ ).

Among the objects with securely determined FWHM for  $[\text{O I}]$  and  $[\text{S II}]$ , approximately 15%–20% of LINERs and 10%

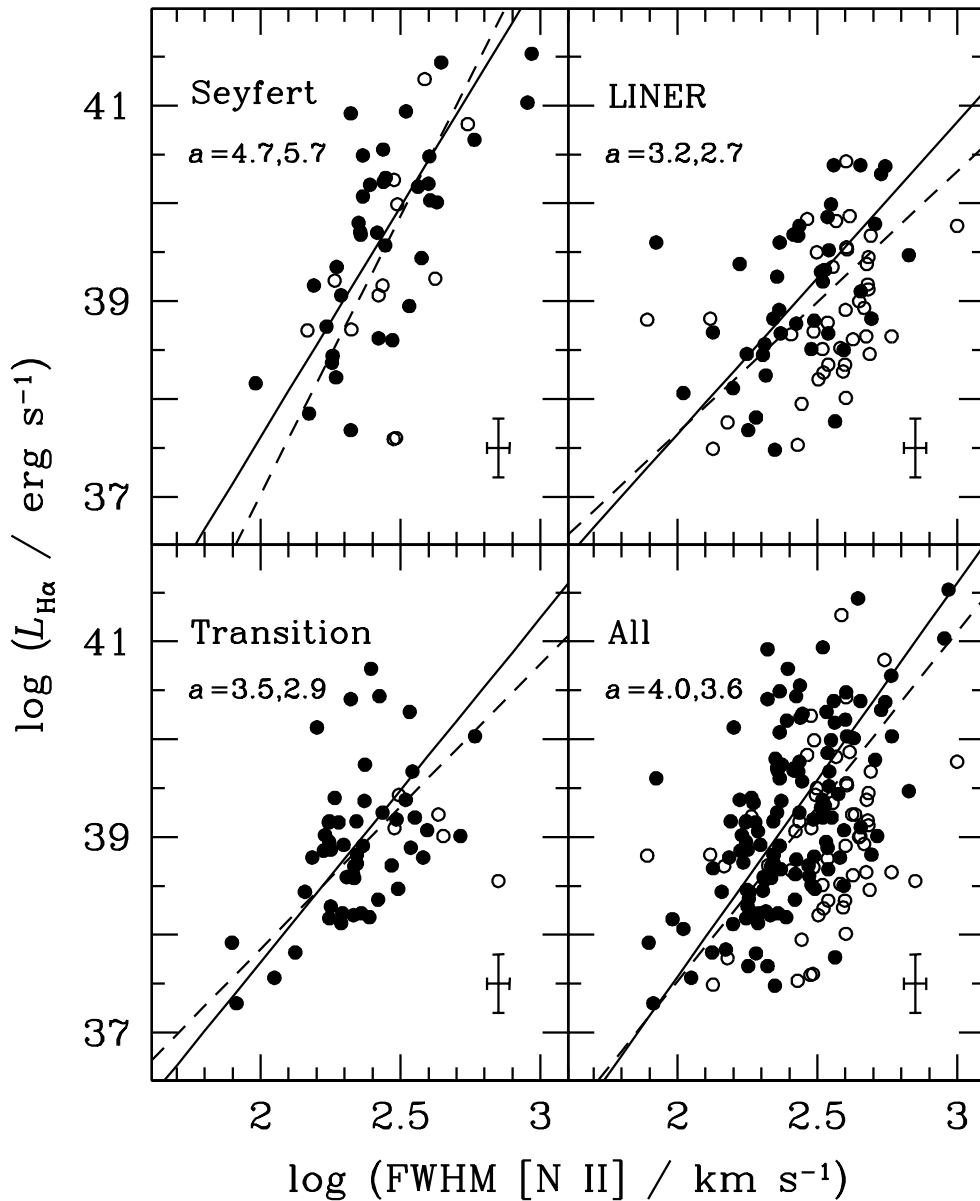


FIG. 8.— Correlation of FWHM of [N II]  $\lambda 6583$  with the luminosity of the narrow  $H\alpha$  line. The line widths have been corrected for instrumental resolution, and the line luminosities have been corrected for extinction. The data are shown in open symbols for the entire sample and in solid symbols for the sample of spirals. In each panel, the linear regression line is plotted; its slope is given in the top left corner. The solid line and the slope listed first correspond to the spiral subsample; the dashed line and the slope listed second refer to the entire sample. Representative error bars are given at the lower right corner of each panel.

of Seyferts show evidence of density stratification in the sense that  $\text{FWHM}([\text{O I}]) > \text{FWHM}([\text{S II}])$  (see Fig. 9 in Ho 1996 for an example). In no instance is [O I] ever observed to be narrower than [S II]. However, these numbers need to be regarded with caution. They do *not* imply that objects failing to show such profile differences lack density stratification, since a number of effects can conspire to hide this observational signature (Whittle 1985c). Furthermore, our ability to discern such subtle profile differences depends strongly on the S/N and resolution of the data, and undoubtedly many objects have escaped notice because of this observational selection effect.

Whittle (1985c) found that Seyfert 1 nuclei have a greater

likelihood of showing profile differences in their forbidden lines than Seyfert 2 nuclei. The implication is that somehow density stratification in the NLR is directly related to the presence of a broad-line region. In the present sample, the same trend seems to hold (see also Ho et al. 1993a), in that, among those objects with detectable profile differences between [O I] and [S II],  $\sim 50\%$  of the LINERs and  $\sim 80\%$  of the Seyferts have broad  $H\alpha$  emission, significantly higher than the respective detection rates of broad  $H\alpha$  in the whole sample (Paper IV). But, once again, this result is difficult to interpret, since selection effects heavily favor the detection of both of these traits in objects having data of high S/N.

TABLE 3A: STATISTICS OF STELLAR POPULATION PARAMETERS

Parameter	Class	Number			Mean			$\sigma$			Median		
		All	Spirals	Sb <sup>a</sup>	All	Spirals	Sb <sup>a</sup>	All	Spirals	Sb <sup>a</sup>	All	Spirals	Sb <sup>a</sup>
$c(44 - 49)$ (mag)	L	92	50	23	0.59	0.58	0.59	0.13	0.16	0.13	0.60	0.58	0.60
	T	63	42	31	0.56	0.56	0.58	0.14	0.15	0.13	0.59	0.59	0.61
	S	52	38	19	0.54	0.54	0.56	0.15	0.15	0.14	0.59	0.59	0.60
	H	201	185	34	0.29	0.29	0.41	0.22	0.22	0.15	0.30	0.31	0.42
	A	66	7	2	0.57	0.48	0.56	0.10	0.13	...	0.59	0.53	...
$c(44 - 66)$ (mag)	L	92	50	23	1.53	1.56	1.55	0.31	0.39	0.30	1.52	1.52	1.55
	T	63	42	31	1.50	1.56	1.59	0.40	0.37	0.34	1.54	1.54	1.57
	S	52	38	19	1.53	1.55	1.63	0.32	0.34	0.34	1.50	1.53	1.59
	H	201	185	34	1.03	1.02	1.32	0.53	0.52	0.39	1.07	1.07	1.32
	A	66	7	2	1.40	1.30	1.48	0.18	0.23	...	1.44	1.38	...
$W(H\beta)$ (Å)	L	92	50	23	2.14	2.39	2.20	0.72	0.78	0.52	1.85	2.31	2.16
	T	61	41	31	2.33	2.42	2.39	0.76	0.78	0.75	2.13	2.34	2.39
	S	43	30	16	2.06	2.05	2.03	0.68	0.56	0.60	1.85	1.86	1.84
	H	189	173	34	3.10	3.09	2.92	0.99	0.94	0.78	2.94	3.00	2.73
	A	66	7	2	2.07	2.34	1.89	0.59	0.68	...	1.89	1.98	...
$W(H\gamma)$ (Å)	L	92	50	23	1.42	1.86	1.57	1.04	1.05	0.71	1.13	1.70	1.64
	T	61	41	31	1.67	1.88	1.84	0.99	0.98	1.02	1.61	1.69	1.76
	S	43	30	16	1.37	1.46	1.47	0.91	0.79	0.86	1.15	1.21	1.16
	H	189	173	34	2.77	2.77	2.54	1.19	1.15	0.99	2.61	2.61	2.31
	A	66	7	2	1.24	1.73	0.90	0.76	1.16	...	1.11	1.45	...
$W(Gband)$ (Å)	L	92	50	23	4.71	4.45	4.77	1.16	1.40	1.02	4.99	4.68	4.89
	T	61	41	31	4.45	4.27	4.34	1.20	1.31	1.25	4.76	4.54	4.45
	S	43	30	16	4.38	4.47	4.87	1.23	1.11	0.84	4.89	4.90	5.03
	H	188	172	34	2.07	2.11	2.48	1.55	1.50	1.45	1.88	1.96	2.53
	A	66	7	2	4.90	4.41	4.89	0.88	1.11	...	5.14	4.52	...
$W(Ca4455)$ (Å)	L	92	50	23	1.52	1.45	1.51	0.37	0.40	0.41	1.59	1.55	1.60
	T	61	41	31	1.48	1.44	1.49	0.38	0.42	0.40	1.53	1.50	1.52
	S	43	30	16	1.54	1.56	1.68	0.39	0.37	0.34	1.61	1.61	1.66
	H	189	173	34	0.77	0.78	0.93	0.44	0.43	0.43	0.73	0.75	0.87
	A	66	7	2	1.65	1.56	1.84	0.41	0.64	...	1.73	1.76	...
$\langle W(Fe) \rangle$ (Å)	L	92	50	23	4.81	4.46	4.65	1.06	1.11	0.96	5.07	4.84	4.99
	T	61	41	31	4.53	4.30	4.49	1.18	1.25	1.19	4.73	4.38	4.52
	S	43	30	16	4.73	4.76	5.18	1.18	1.13	0.91	4.87	4.77	4.97
	H	189	173	34	2.28	2.31	2.73	1.21	1.17	1.22	2.12	2.16	2.64
	A	66	7	2	5.04	4.70	5.64	1.04	1.62	...	5.14	5.42	...

NOTE.—Class “A” refers to absorption-line nuclei.  
<sup>a</sup>Hubble types Sab–Sbc ( $T = 2 - 4$ ).

### 2.5. Nuclear Stellar Content

Paper III gives several parameters that are useful indicators of the nuclear stellar population, at least in a statistical and relative sense. These are summarized in Table 3a, and comparisons between the different classes of objects are given in Table 3b. To a first approximation, the three AGN subtypes reveal no statistical differences in their nuclear stellar content, especially after isolating the spiral and Sb subsample. This is reflected in the spectrophotometric colors [ $c(44 - 49)$  and  $c(44 - 66)$ ] and in the Balmer and metal-line absorption features. Figure 9 plots the age-sensitive indices,  $W(H\beta)$  and  $W(H\gamma)$  against the metallicity-sensitive indices,  $\langle W(Fe) \rangle$  and  $W(Ca4455)$ . All three classes of AGN nuclei overlap considerably, and there are no noteworthy differences among them (Table 3b). We have also examined the behavior of the G band near 4300 Å, and it, too, is very homogeneous among the three classes.

As expected, H II nuclei occupy a distinctly different locus with respect to the AGN nuclei. They have strong Balmer lines and weak metal lines — signatures of a young to intermediate-

age stellar population — consistent with the expectation that the emission-line spectrum of H II nuclei is powered predominantly by young, massive stars.

Table 3a also lists the statistics for the absorption-line nuclei (nuclei with no detectable emission lines) from the Palomar survey. Most of the galaxies are ellipticals and lenticulars, which have characteristically old stellar populations. The statistics for the spiral and Sb subsamples are limited, but they do not appear to be grossly dissimilar from those of the whole sample. It is striking that both the absorption-line nuclei and the three classes of active nuclei have such closely matching stellar population parameters. We can infer, from this comparison, that an old stellar population prevails in most LINER, transition, and Seyfert nuclei.

## 3. DISCUSSION

### 3.1. The Origin of the Low-Ionization State in LINERs

While there is now abundant evidence that a significant fraction of LINERs are accretion-powered sources [see recent reviews by Ho (1999a, 2002) and Barth (2002)], it is still unclear

TABLE 3B: COMPARISON OF STELLAR POPULATION PARAMETERS

Parameter	Test	L/T	L/S	L1/L2	S1/S2	L+T+S/H
$c(44 - 49)$	$P_K$	0.983	0.780	0.994	0.797	$<1 \times 10^{-5}$
	$P_G$	0.589	0.486	0.769	0.529	$<1 \times 10^{-5}$
	$P_t$	0.678	0.506	0.393	0.649	$<1 \times 10^{-5}$
$c(44 - 66)$	$P_K$	0.950	0.999	0.654	0.0435	$2.9 \times 10^{-4}$
	$P_G$	0.700	0.643	0.734	0.0592	$2.0 \times 10^{-4}$
	$P_t$	0.624	0.445	0.465	0.289	$8.3 \times 10^{-4}$
$W(\text{H}\beta)$	$P_K$	0.261	0.234	0.594	0.0463	$8.7 \times 10^{-4}$
	$P_G$	0.419	0.121	0.287	0.0502	$1.0 \times 10^{-4}$
	$P_t$	0.298	0.352	0.375	0.0351	$5.8 \times 10^{-5}$
$W(\text{H}\gamma)$	$P_K$	0.812	0.137	0.255	0.315	$2.0 \times 10^{-4}$
	$P_G$	0.569	0.311	0.287	0.179	$<1 \times 10^{-5}$
	$P_t$	0.246	0.711	0.356	0.0871	$5.5 \times 10^{-5}$
$W(\text{Gband})$	$P_K$	0.267	0.937	0.957	0.507	$<1 \times 10^{-5}$
	$P_G$	0.202	0.909	0.799	0.897	$<1 \times 10^{-5}$
	$P_t$	0.176	0.747	0.482	0.303	$<1 \times 10^{-5}$
$W(\text{Ca4455})$	$P_K$	0.375	0.590	0.886	0.924	$<1 \times 10^{-5}$
	$P_G$	0.398	0.272	0.743	0.843	$<1 \times 10^{-5}$
	$P_t$	0.818	0.181	0.972	0.487	$<1 \times 10^{-5}$
$\langle W(\text{Fe}) \rangle$	$P_K$	0.368	0.438	0.981	0.507	$<1 \times 10^{-5}$
	$P_G$	0.425	0.231	0.824	0.253	$<1 \times 10^{-5}$
	$P_t$	0.587	0.0877	0.719	0.114	$<1 \times 10^{-5}$

NOTE.—The two-sample tests are restricted to the subsample of Sab–Sbc galaxies, with the exception of the comparisons between type 1 and type 2 objects (L1/L2 and S1/S2), which use the entire sample of spirals.  $P_K$  and  $P_G$  are the probabilities for rejecting the hypothesis that two samples are drawn from the same parent population according to the Kolmogorov-Smirnov and Gehan’s generalized Wilcoxon tests, respectively. Student’s  $t$  test ( $P_t$ ) evaluates the null hypothesis that two samples have the same mean. The subclasses of emission-line objects follow the notation of Paper III, where H = H II nucleus, L = LINER, T = transition object (LINER/H II nucleus), S = Seyfert, and “1” and “2” denote type 1 and type 2 nuclei, respectively.

what physical parameters actually determine the low-ionization state in LINERs. In the context of AGN photoionization, the optical signature of LINERs has been primarily attributed to a low ionization parameter,  $U$ , defined as the ratio of the density of ionizing photons to the density of nucleons at the illuminated face of a cloud. Whereas the NLR spectrum of Seyferts can be well reproduced with  $\log U \approx -2.5 \pm 0.5$  (e.g., Ferland & Netzer 1983; Stasińska 1984; Ho, Shields, & Filippenko 1993b), that of LINERs requires  $\log U \approx -3.5 \pm 1.0$  (Ferland & Netzer 1983; Halpern & Steiner 1983; Péquignot 1984; Binette 1985; Ho et al. 1993a). What factors contribute to the lower ionization parameters in LINERs?

The ionization parameter is conventionally related to the physical parameters of a line-emitting region by the expression  $U = Q_{\text{H}} / (4\pi r^2 n c)$ , where  $Q_{\text{H}}$  is the number of ionizing photons  $\text{s}^{-1}$ ,  $n$  is the gas number density, and  $r$  is the distance between the central ionizing source and the illuminated cloud. Recasting the structure of the nebula in terms of a volume filling factor  $\epsilon$ ,  $U \propto (Q_{\text{H}} n \epsilon^2)^{1/3}$ . Unfortunately, our observations do not constrain  $\epsilon$ . We can, however, estimate the remaining two variables, since  $Q_{\text{H}} \propto L_{\text{H}\alpha}$  in an ionization-bounded nebula and  $n \approx n_e$ . From § 2.3, we know that LINERs are intrinsically less powerful sources than Seyferts; the typical  $\text{H}\alpha$  luminosities differ by approximately an order of magnitude. On the other hand, the electron densities in LINERs are lower than those in Seyferts by a factor of  $\sim 3$ . Thus, neglecting for the moment possible systematic variations in  $\epsilon$  between the two classes, we expect

LINERs to have values of  $U$  that are, on average, lower by  $\sim 30^{1/3}$ , or  $\sim 3$ . While this does not fully reconcile the factor of 10 difference in  $U$  between LINERs and Seyferts, it is the first direct demonstration that systematic variations in nebular conditions may be responsible for the spectral distinction between low-ionization and high-ionization AGNs.

Clearly, further progress would require data on  $\epsilon$ , especially in view of its relatively strong influence on  $U$ . For the central photoionization picture to remain viable, the emission nebulae in LINERs should have lower volume filling factors than in Seyferts, on average by a factor of a few. Observational constraints on  $\epsilon$  can be derived from knowledge of the size of the NLR, in conjunction with its line luminosity and density. The ground-based narrow-band imaging surveys of Keel (1983b) and Pogge (1989a), which included a number of nearby LINERs, find that the majority of them have fairly compact, centrally concentrated NLRs. The emission cores are generally unresolved or only marginally resolved under  $1''$ – $2''$  seeing. This result has been verified for a limited sample of 14 LINERs imaged with the *Hubble Space Telescope* (*HST*): the bulk of the line emission is confined to size scales of tens to hundreds of parsecs (Pogge et al. 2000). The compact morphology of the NLRs in LINERs ostensibly seems to differ from the extended emission-line structures and ionization cones commonly associated with Seyfert galaxies (e.g., Pogge 1989b; Mulchaey, Wilson, & Tsvetanov 1996). However, one must regard this comparison with some caution. Past emission-line

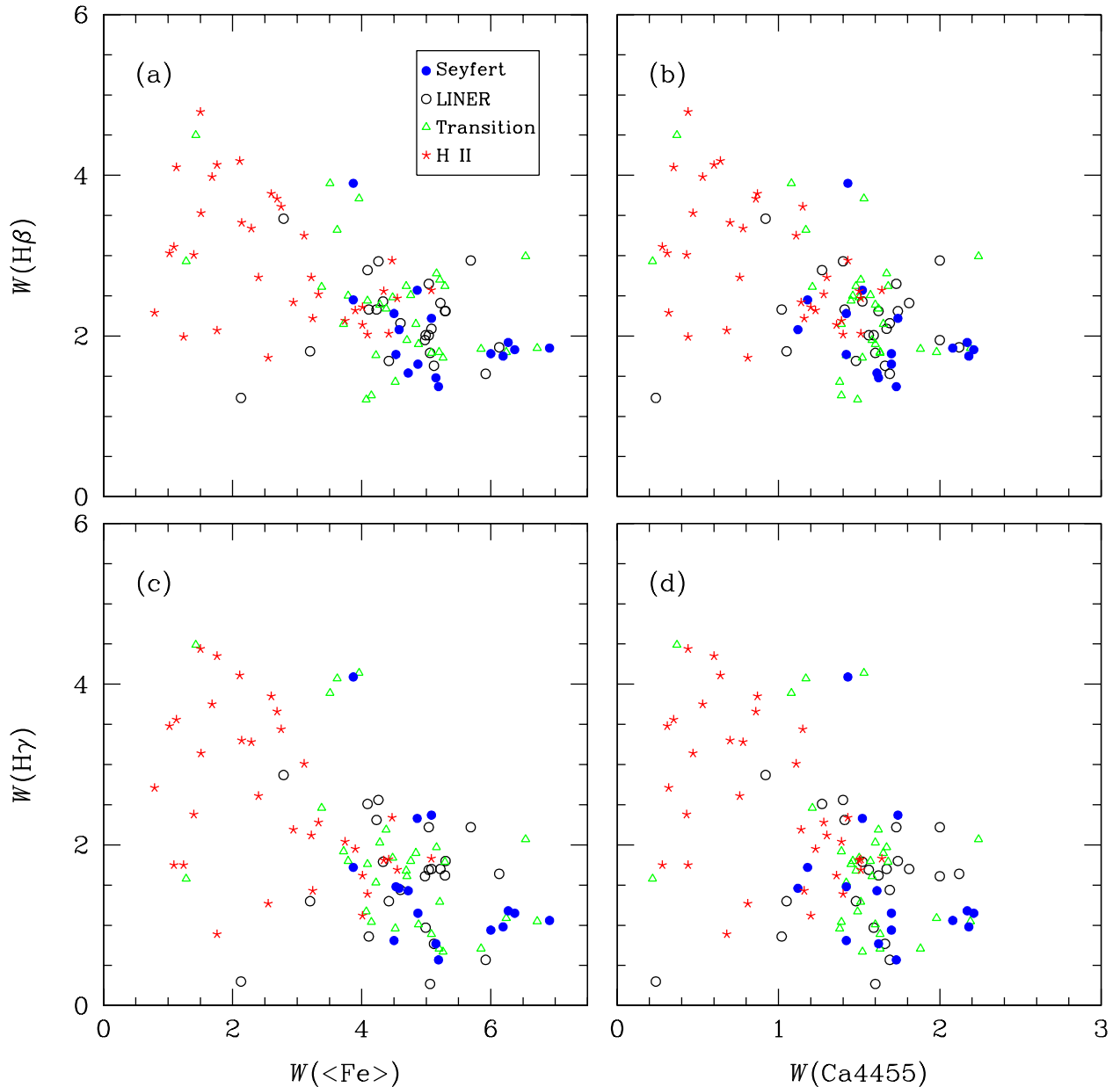


FIG. 9.— Stellar absorption indices indicative of the age [ $W(\text{H}\beta)$  and  $W(\text{H}\gamma)$ ] and metallicity [ $\langle W(\text{Fe}) \rangle$  and  $W(\text{Ca4455})$ ] of the stellar population, as defined in Paper III, for Seyferts (solid circles), LINERs (open circles), transition objects (triangles), and H II nuclei (stars). Only Sab–Sbc galaxies are included.

imaging studies have targeted Seyferts that are generally much more luminous than the “garden-variety” sources represented in the Palomar survey. If the linear extent of the NLR correlates with line luminosity, as found by Mulchaey et al. (1996), it is possible that the majority of nearby Seyferts have more compact NLRs than previously believed. The work of Keel (1983b) tentatively supports this hypothesis. The majority of the galaxies in Keel’s study overlap with the Palomar survey, and thus can be spectroscopically classified according to our system. In all, there are six Seyferts and 15 LINERs, and the average seeing-corrected FWHM sizes of the  $\text{H}\alpha + [\text{N II}]$  emis-

sion regions are, respectively,  $4.4''$  and  $3.5''$ . These statistics are clearly too limited to be definitive, but they illustrate that the NLRs of nearby (low-luminosity) Seyferts may indeed be quite compact. It would be desirable to address these issues by conducting a high-resolution imaging survey of the Palomar LINERs and Seyferts matched in line luminosity and Hubble type.

A common theme echoed throughout this paper is that LINERs and Seyferts share, perhaps surprisingly, a large number of traits. After factoring out slight differences in Hubble type distribution, the global properties of their host galaxies are vir-

tually identical. The distinguishing features that emerge all pertain to the circumnuclear environment: LINERs have lower gas densities and less internal reddening relative to Seyferts. This suggests that the central regions of LINERs have characteristically lower amounts of cold interstellar material. It is reasonable to speculate that the lower circumnuclear gas content may lead to a reduction in the gas reservoir available to fuel the central engine, which in turn explains the observed lower luminosity output.

A sizable reduction in accretion rate can have other consequences. Several recent studies have remarked that the broad-band spectral energy distributions of low-luminosity AGNs, particularly LINERs, are systematically different from those of higher luminosity sources such as classical Seyfert 1 nuclei and quasars (Ho 1999b, 2002; Ho et al. 2000). The most salient feature is a marked deficit of optical and ultraviolet (UV) photons normally attributed to thermal emission from an optically thick, geometrically thin accretion disk. As suggested by Ho (2002), this modification of the spectral energy distribution hardens the ionizing radiation field, which, all else being equal, boosts the strengths of the low-ionization lines. This effect, however, is likely to be only secondary compared to the variation in ionization parameter.

### 3.2. *The Role of Shocks*

The relevance of shocks to the excitation of LINERs has been a topic of ongoing debate ever since LINERs were first identified (Koski & Osterbrock 1976; Fosbury et al. 1978; Heckman 1980; Dopita & Sutherland 1995; Alonso-Herrero et al. 2000; Sugai & Malkan 2000). Optical emission-line diagnostics, unfortunately, do not discriminate well between shocks and conventional AGN photoionization. Although the UV region offers more promise, according to the fast-shock ( $v \approx 150 - 500 \text{ km s}^{-1}$ ) models of Dopita & Sutherland (1995), to date none of the LINERs that have been studied spectroscopically in the UV using the *HST* have revealed the predicted strong high-excitation UV lines (see summary in Ho 1999a, and references therein)<sup>3</sup>. The present work has some relevance to the issue of shocks. From analysis of the line profiles (§ 2.4), we find that the nuclear ionized gas in LINERs and Seyferts have comparable velocity dispersions; depending on Hubble type,  $100 \lesssim v_{\text{gas}} \lesssim 170 \text{ km s}^{-1}$ , where  $v_{\text{gas}} = 0.5 \text{ FWHM}([\text{N II}])$ . Now, in spiral galaxies at least part of the line width observed through a ground-based aperture must come from spatially unresolved rotation of the inner disk, and so the true random, cloud-cloud impact velocities should be less than  $v_{\text{gas}}$ . Even so, these velocities already fall considerably short of the values assumed in fast-shock models. Moreover, if LINERs are preferentially shock excited, one would naively expect their internal gas motions to be higher than in Seyferts, contrary to what is observed. In fact, judging by the frequency with which asymmetric narrow-line profiles are observed in LINERs, as well as the clear preference for the asymmetry to occur blueward of the line center, the bulk velocity field of their NLRs appears to be remarkably similar to that of Seyferts.

### 3.3. *The Role of Stellar Photoionization and the Nature of Transition Objects*

Beginning with the work of Terlevich & Melnick (1985), there have been a number of attempts to invoke photoionization by hot, young stars as the primary source of excitation for LINERs and related objects. As with the shock models discussed above, the main motivation for the stellar-based models is clear: if alternatives to AGN photoionization can be found to give a satisfactory explanation of LINERs, then LINERs should not be regarded as AGNs. Filippenko & Terlevich (1992) and Shields (1992) showed that the primary optical spectral features of transition objects<sup>4</sup> can be reproduced by photoionization by O-type stars having effective temperatures  $\gtrsim 45,000 \text{ K}$  embedded in an environment with high density and low ionization parameter. Taniguchi, Shioya, & Murayama (2000) advocate that the ionization source for LINERs can be supplied by a cluster of planetary nebula nuclei formed 100–500 Myrs following a nuclear starburst.

An improved treatment of the problem studied by Filippenko & Terlevich (1992) and Shields (1992) was recently presented by Barth & Shields (2000), who modeled the ionizing source not as single O-type stars but as a more realistic evolving young star cluster. Barth & Shields confirm that young, massive stars can indeed generate optical emission-line spectra that match those of transition objects, but only under the following conditions: the cluster needs to be formed in an instantaneous burst, its metallicity should be solar or greater, and its age must lie in the narrow range  $\sim 3 - 5 \text{ Myr}$ . The latter restriction ensures that there are sufficient Wolf-Rayet (W-R) stars available to supply the extreme-UV photons necessary to boost the low-ionization lines. As Barth & Shields emphasize, however, simple considerations of the demographics of emission-line nuclei observed in the Palomar survey (Paper V) indicate that the starburst model is unlikely to apply to most transition objects, especially those hosted by earlier-type galaxies.

The models of Barth & Shields (2000) also succeed in explaining the optical spectra of bona fide LINERs, again provided that the starburst is caught during the brief phase when W-R stars exist. To achieve consistency with the relative strengths of [O I], [N II], and [S II] observed, the models additionally require above-solar metallicities and the coexistence of a high-density and a low-density component, similar to the scenario envisioned by Shields (1992). As with the transition objects, however, the starburst model for LINERs appears to be applicable only to late-type galaxies, which host only a small fraction of the known LINERs.

As recognized by Barth & Shields (2000), the critical role played by W-R stars in their model presents a somewhat perplexing problem: why do LINERs and transition objects almost never show W-R features (e.g., the broad “bump” near  $4650 \text{ \AA}$ ) in their spectra? Conversely, why do galaxies with detected W-R features (“W-R galaxies”; see Conti 1991) seldom qualify as LINERs or transition objects according to their narrow-line spectra? Since W-R features are recognized most commonly, and perhaps selectively, in late-type galaxies, Barth & Shields (2000) speculate that the absence of LINER-like spectra in W-R galaxies may be a consequence of their low metallicity, and possibly low density. They attribute the apparent rarity of the W-R bump in LINERs and transition nuclei to the difficulty of detecting this weak, broad feature in the presence of strong starlight contamination from the bulge of the host galaxy. We do not

<sup>3</sup> The case discussed by Dopita et al. (1997) concerns the circumnuclear *disk* of M87, not the nucleus itself. Sabra et al. (2002) show that the UV–optical spectrum of the nucleus of M87 is best explained by a multi-component photoionization model.

<sup>4</sup> Filippenko & Terlevich (1992) and Shields (1992) refer to these sources as “weak-[O I] LINERs,” but they are equivalent to transition objects.

believe this to be the case. While contamination from the underlying bulge stars indeed does pose a serious challenge to detecting weak emission lines in galactic nuclei, all emission-line measurements from the Palomar survey were done *after* careful starlight subtraction (Paper III). To be sure, the correction for starlight was not perfect in all cases, especially for objects with extremely weak emission lines. Nonetheless,  $H\beta$  emission is detected unambiguously in the vast majority of the LINERs and transition nuclei in the Palomar survey. Furthermore, the starlight-subtracted spectra in the region of the W-R bump ( $\sim 4600\text{--}4700\text{ \AA}$ ) have residuals comparable to that of the continuum near  $H\beta$ . For high ( $\gtrsim$  solar) metallicities, the strength of the W-R bump is expected to be comparable to, if not greater than, that of  $H\beta$  (Schaerer & Vacca 1998). It is thus hard to imagine how it could have been missed, especially considering the size of the Palomar sample ( $\sim 160$  LINERs and transition objects).

Are there other indications that low-ionization nuclei contain young stars? The two best examples are NGC 404 (a LINER) and NGC 4569 (a transition object). Both objects have a prominent nuclear star cluster detected in *HST* UV images (Maoz et al. 1995; Barth et al. 1998), and follow-up spectroscopy reveals that the UV light is dominated by emission from massive, young stars (Maoz et al. 1998). Although the youth of the nuclear stellar population in NGC 404 and NGC 4569 manifests itself most dramatically in the UV, it is also unmistakable in the optical. The blue Palomar spectra of these two objects (Paper II) show extremely prominent  $H\gamma$  and  $H\beta$  absorption lines. We measure  $W(H\gamma) = 3.4$  and  $4.5\text{ \AA}$  and  $W(H\beta) = 3.6$  and  $4.5\text{ \AA}$  for NGC 404 and NGC 4569, respectively. The metal lines are correspondingly weakened by dilution from the continuum of hot stars. The respective indices for NGC 404 and NGC 4569 are  $W(\text{Gband}) = 1.8$  and  $0.74\text{ \AA}$ ,  $W(\text{Ca4455}) = 0.68$  and  $0.37\text{ \AA}$ , and  $W(\text{Fe}) = 2.3$  and  $1.4\text{ \AA}$ . The vast majority of LINERs and transition nuclei, however, do *not* resemble NGC 404 and NGC 4569. UV-bright nuclei, whether stellar or nonstellar, occur in only  $\sim 20\text{--}25\%$  of nearby AGNs (Maoz et al. 1995; Barth et al. 1998). More striking still, as shown in § 2.5, active nuclei in nearby galaxies, irrespective of spectral classification, contain predominantly *old* stellar populations. The optical stellar indices of NGC 404 and NGC 4569 (given above) are highly unrepresentative of the bulk of LINERs and transition nuclei of similar Hubble type (see Table 3a).

How confident are we that young stars cannot be present in significant numbers? Perhaps the number of young stars required to drive the emission lines would be imperceptible in the presence of the more abundant old stars. To evaluate this possibility, consider the following. The average  $H\alpha$  luminosity of LINERs and transition objects,  $\sim 3 \times 10^{39}\text{ erg s}^{-1}$ , if generated under Case B recombination, corresponds to an ionizing photon rate of  $\sim 3 \times 10^{51}\text{ s}^{-1}$ . If the ionization can be entirely attributed to an ongoing starburst, say at an age of 5 Myr, we estimate from the models of Leitherer et al. (1999) that the associated stellar component has an absolute  $B$ -band magnitude of  $M_B \approx -14.5$  mag. We have chosen the calculations that assume solar metallicity and a Salpeter stellar initial mass function with an upper-mass cutoff of  $100 M_\odot$ . This can be directly compared to the nuclear optical magnitudes compiled in Paper III, which were derived from our spectrophotometric measurements. The average monochromatic absolute magnitude at

$4400\text{ \AA}$  is  $\langle M_{44} \rangle = -16.1$  mag for LINERs and  $\langle M_{44} \rangle = -15.5$  mag for transition nuclei. The starburst component, if present, would comprise  $\sim 25\text{--}40\%$  of the observed  $B$ -band light, and thus should be readily detectable.

The above considerations cast doubt on the general applicability of models that seek to account for the excitation of LINERs and transition nuclei using young stars. Models that rely on a starburst rich in W-R stars, such as that by Barth & Shields (2000), face the puzzle that W-R stars are rarely detected in these systems. Post-starburst models (e.g., Taniguchi et al. 2000) bypass this problem, but like the starburst models, they cannot escape the predicament that the nuclear stellar population is demonstrably old.

Ho et al. (1993a) originally proposed that transition objects are composite in nature, namely systems consisting of a “normal” LINER nucleus whose signal has been diluted by neighboring, circumnuclear H II regions, or simply by H II regions projected along the line of sight into the spectroscopic aperture. This seems to be the most natural explanation for their location, sandwiched between H II regions and LINERs, in optical line-ratio diagrams. A similar argument, based on decomposition of line profiles, has been made by Véron, Gonçalves, & Véron-Cetty (1997) and Gonçalves, Véron-Cetty, & Véron (1999). As noted in Paper V and in § 2.1, the overall distribution of Hubble types for transition objects tends to be skewed toward later morphologies. This is not unexpected, to the extent that star formation is more prevalent in later type galaxies. More intriguingly, we find that the host galaxies of transition nuclei seem to exhibit systematically higher levels of recent star formation compared to LINERs of *matched* morphological types (i.e., within the Sb subsample). This is suggested by the higher  $L_{\text{FIR}}/L_B^0$  ratios and mildly bluer broad-band optical colors in transition objects. Since these are spatially unresolved measurements, however, we do not know the location of the enhanced star formation. Moreover, we showed that the host galaxies of transition nuclei also have a tendency to be slightly more inclined than LINERs. Thus, all else being equal, transition-type spectra seem to be found precisely in those galaxies whose nuclei have a high probability of being contaminated by extra-nuclear emission from star-forming regions.

The above proposition, it may be argued, seems to be at odds with the stellar population of transition nuclei. If star-forming regions contribute significantly to the integrated nuclear emission of transition objects, then why is there no strong evidence that they have a younger population than LINERs<sup>5</sup>? This apparent inconsistency perhaps can be resolved by recognizing that in giant H II regions the line-emitting regions can be considerably more extended than, and often offset from, the stellar continuum sources (see, e.g., Whitmore et al. 1999; Maoz et al. 2001). A spectroscopic aperture, therefore, can intercept significant line emission from near-nuclear or projected H II regions without admitting much of the associated continuum light.

### 3.4. The Role of Interactions

The influence of the local environment on nuclear activity is not the primary subject of this investigation, but our analysis touches upon a few items relevant to this issue. Although tidal interactions have been well demonstrated to have an important influence on nuclear star formation, their influence on AGN activity, albeit often implicated in the literature, is far from

<sup>5</sup> The stellar population parameters of transition nuclei indeed *do* indicate systematically younger ages than LINERs (Table 3a), but the differences are not large enough to be statistically significant.

clear. This is especially true of lower luminosity AGNs such as Seyfert nuclei (see Combes 2001, and references therein).

Statistical studies of this type are at the mercy of selection effects and sample biases. In this respect, the Palomar survey has a number of merits, as emphasized by Ho & Ulvestad (2001). Schmitt (2001), taking advantage of this fact, has studied the frequency of companions for galaxies with different nuclear types in the Palomar survey. The approach taken by Schmitt is very similar to ours. He evaluates the influence of companion galaxies using  $\rho_{\text{gal}}$  taken from Paper III and a parameter equivalent to, but quantitatively slightly different from,  $\theta_p$ . A galaxy is considered to have a companion if another galaxy with a magnitude difference of  $\pm 3$  mag and a velocity difference of  $\pm 1000$  km s<sup>-1</sup> is found within a separation of  $5 D_{25}$  of the primary. By either measure, Schmitt concludes that the local environment has no correlation with the activity type, as long as one properly accounts for the morphology-density relation. This is precisely what we found in § 2.2. Thus, although non-axisymmetric perturbations from galaxy interactions may be effective in driving gas from galactic scales ( $\sim 10$  kpc) to the circumnuclear region ( $\sim 0.1 - 1$  kpc), wherein nuclear starbursts may ignite (e.g., Barnes & Hernquist 1991), the gas evidently has more trouble dissipating to scales pertinent to feeding a central black hole ( $\lesssim 1$  pc). Ho et al. (1997d) arrived at the same conclusion in considering the effect of bars on nuclear activity found in the Palomar survey. Schmitt notes that the null effect of companions on AGN fueling cannot be easily dismissed by appealing to the low level of activity represented by the Palomar objects. The frequency of companions for the Palomar Seyferts appears to be comparable to that in the much more luminous sample studied by Schmitt et al. (2001).

### 3.5. Seyfert Galaxies: Not So Unified?

According to the simplest version of AGN unification (see, e.g., Antonucci 1993; Wills 1999), type 2 Seyferts are intrinsically the same as type 1 Seyferts, but viewed from an angle in which a small-scale dusty “torus” obscures its broad-line region. For this picture to hold, we expect both types to have similar isotropic properties. As before, here it is of paramount importance to minimize potential selection effects, which traditionally have plagued analyses of this kind. The Palomar sample is again quite valuable in this regard. Its main disadvantage is the small size; when the analysis is confined to the spiral galaxies, there are only 18 Seyfert 1s and 20 Seyfert 2s. Nonetheless, some trends are apparent.

As can be seen from Table 1b, the host galaxy parameters of both types of Seyferts are mostly well matched, with the following exception. Relative to Seyfert 2s, Seyfert 1s have comparable FIR emission (normalized to the optical) but *hotter* FIR colors (higher  $S_{60}/S_{100}$  and  $S_{25}/S_{60}$  ratios). Models of optically thick obscuring tori (e.g., Pier & Krolik 1992; Efstathiou & Rowan-Robinson 1995) predict a significant degree of anisotropy for the infrared emission, such that face-on tori should be hotter than edge-on tori. The systematic differences in FIR colors are therefore in qualitative agreement with the model predictions. Heckman (1995), by comparing the ratio of  $10 \mu\text{m}$  emission to 1.4 GHz and [O III]  $\lambda 5007$  luminosity in broad-line versus narrow-line AGNs, also concluded that the mid-infrared emission must be emitted anisotropically.

In terms of nuclear properties, we find that Seyfert 1s tend to have weaker stellar indices than Seyfert 2s. This result is simple to understand in terms of dilution by the stronger feature-

less continuum in Seyfert 1s, because relative to Seyfert 2s they have a more dominant, directly viewed AGN component compared to the underlying galaxy. Although both Seyfert types have similar narrow-line H $\alpha$  luminosities (Table 2b), the total (narrow plus broad) line luminosity of Seyfert 1s is higher than that of Seyfert 2s. Thus, this result does not conflict with the unified model either.

Two points, however, are less straightforward to grasp. Taken at face value, they appear to violate the simplest formulation of the unified model. First, as mentioned in § 2.2, Seyfert 1s seem to prefer environments of higher galaxy density than Seyfert 2s. Since both subsamples are well matched in Hubble type and total galaxy luminosity, we cannot dismiss it by appealing to the morphology-density effect. Second, Seyfert 1s have statistically higher NLR electron densities than Seyfert 2s. Their density distributions differ at the level of  $P_K = 3\%$  and  $P_G = 1\%$ , while the difference in their means ( $632$  and  $380$  cm<sup>-3</sup>, respectively) is significant at the level of  $P_t = 0.8\%$ .

The following complication, however, might obviate the above apparent inconsistency with the unified model. The spectral classifications in the the Palomar survey, as in all large spectroscopic surveys, are based on integrated-light spectra, with no means of distinguishing scattered emission from direct emission. The Palomar survey contains a large number of objects with very weak broad lines, many classified as type 1.8 or type 1.9 sources. For these objects, we do not know for sure whether the broad-line emission is viewed directly or is largely reflected into our line of sight. If the latter is true, as in the case of NGC 1068 (Antonucci & Miller 1985), then such objects should be classified as type 2 rather than type 1 objects. Sensitive spectropolarimetric observations of the Palomar Seyferts are needed before they can be used to definitively test the unified model.

### 3.6. What “Activates” Galactic Nuclei?

Dynamical studies suggest that most, perhaps all, galactic bulges contain massive black holes (Magorrian et al. 1998; Gebhardt et al. 2002). Insofar as AGNs signify black hole accretion, AGN surveys can serve as an alternative and efficient tool to assess black hole demographics. As noted by Ho (2002), the high AGN fraction among bulge-dominated galaxies in the Palomar survey ( $\gtrsim 50\%$ – $75\%$  for E–Sbc galaxies) supports the idea that black holes are ubiquitous in bulges. What about the small, but still sizable, minority of bulged galaxies that are classified as H II nuclei? Why are they “inactive”? One possibility is that they lack black holes. A more mundane alternative, however, is that the AGN signal is simply swamped by the much more dominant light from the H II regions. Among Sb galaxies, for instance, the H $\alpha$  luminosity of H II nuclei easily rivals that of Seyferts and typically exceeds that of LINERs and transition objects by an order of magnitude. If this scenario is correct, we expect that spectra taken at high spatial resolution would look progressively more AGN-like.

Table 1 shows that the host galaxies of H II nuclei tend to be slightly richer in atomic hydrogen compared to the host galaxies of AGNs, although we know little of the internal distribution of the gas. The higher gas content plausibly leads to elevated star formation, both on nuclear scales, as reflected in the spectral classification, and on galaxy-wide scales, as indicated by the integrated optical colors and FIR properties. An additional trend is noteworthy. For a given Hubble type, H II nuclei are preferentially found in galaxies of somewhat lower total optical luminosity; they tend to be less luminous than AGN hosts

by  $\sim 0.3-0.4$  mag. This is probably just a consequence of the inverse correlation between gas content and optical luminosity in spiral galaxies (Roberts & Haynes 1994). The systematically lower luminosities account for the more compact isophotal diameters (Holmberg 1975) and reduced bulge luminosities, which depend directly on the total luminosities.

With the knowledge that all bulges are likely to contain massive black holes, and therefore the necessary condition to host AGNs, the longstanding, unanswered question of what triggers the activity becomes even more acute. Apparently, the mere availability of gas on circumnuclear scales — inferred from the strong line emission and high internal reddening in H II nuclei — is not sufficient; most of the gas never gets accreted, hence leading to the low level of activity that we speculate lies masked by the H II regions. The key issue, then, is what factors predispose a galactic nucleus to convert most of its gas into stars instead of funneling it to feed the central engine. Environment seems to matter little, as discussed in § 3.4. On nuclear scales, the density of the gas, at least in the warm ionized phase, is not grossly different between AGN and non-AGN hosts. The most disparate trait between the two samples is the width of the emission lines. Among Sb galaxies,  $\langle \text{FWHM}([\text{N II}]) \rangle = 164 \text{ km s}^{-1}$  for H II nuclei, whereas  $\langle \text{FWHM}([\text{N II}]) \rangle = 258 \text{ km s}^{-1}$  for LINERs, transition objects, and Seyferts combined; the two samples differ at a very high level of significance ( $P_K \approx P_G \approx P_I \lesssim 10^{-5}$ ; Table 2*b*). The slight difference in total or bulge luminosity between the two groups cannot account for such a large difference in line widths. The gas in the central regions of galaxies hosting H II nuclei is *kinematically colder* than in galaxies that host active nuclei. Expressed in another way, the gas surrounding H II nuclei has higher angular momentum than the gas in AGN nuclei. Thus, the angular momentum content of the circumnuclear gas may be the critical factor that determines whether material can be channeled to the center for AGN fueling.

#### 4. SUMMARY

We have used the database assembled in Paper III to quantify statistically the global and nuclear properties of the various subclasses of emission-line nuclei found in nearby galaxies. To mitigate spurious results that can arise from differences in Hubble type distribution, we have focused our attention on a restricted set of Sab–Sbc galaxies. The main results can be summarized as follows.

1. The host galaxies of LINERs, transition nuclei, and Seyferts have fairly uniform large-scale properties. The most notable exception is that transition objects, relative to LINERs, tend to be somewhat more highly inclined and show mild evidence for enhanced star formation.
2. The nebular parameters of LINERs are broadly similar to those of transition nuclei, but they differ quite dramatically from those of Seyferts. Seyfert nuclei tend to have significantly stronger line emission, denser gas, and higher levels of internal reddening. These trends suggest that Seyferts have more gas-rich circumnuclear environments, and plausibly larger accretion rates, than LINERs.
3. The characteristically lower nuclear luminosities and densities of LINERs compared to Seyferts can partly account for the difference in ionization parameter between these two classes of objects.
4. The line-emitting regions in LINERs and Seyferts share very similar kinematics. This is reflected both in their line widths and profile asymmetries. Transition objects, by contrast, exhibit markedly narrower emission lines, presumably because a greater fraction of its ionized gas has disklike kinematics. All three classes obey a correlation between line luminosity and line width, approximately of the form  $L \propto \text{FWHM}^a$ , with  $a \approx 3-4$ .
5. Based on the modest gas velocity dispersions observed in LINERs and Seyferts, as well as their similarity between the two classes of objects, we argue that fast shocks are unlikely to be an important contributor to the excitation of LINERs.
6. The central regions of most nearby AGNs have uniformly old stellar populations. We show that this poses a serious obstacle to models that invoke young stars as the primary energy source to power the emission lines.
7. The hypothesis that transition objects are composite LINER/H II nuclei remains viable as long as the H II region component does not contribute appreciably to the measured stellar continuum.
8. Consistent with other recent studies, we find that the local environment, as measured through either the local galaxy density or the distance to the nearest sizable companion, has a negligible effect on the general spectral class of emission-line nuclei (Seyferts, LINERs, or transition objects).
9. Type 1 and type 2 Seyferts have largely, but not completely, similar global and nuclear properties. Two of the differences between the two types, as reflected in the local environment of the host galaxies and in the electron densities of the emission-line regions, may present a challenge for unification models for Seyfert galaxies.
10. The primary trait that distinguishes AGN and non-AGN host galaxies on small scales appears to be the velocity field of the nuclear gas. The line-emitting gas in H II nuclei is systematically kinematically colder, and hence has higher angular momentum, than the gas in active nuclei. We suggest that the angular momentum content of the nuclear gas may be a critical factor that determines whether gas can flow to the center to feed an AGN.

This research is funded by the Carnegie Institution of Washington, by NASA grants from the Space Telescope Science Institute (operated by AURA, Inc., under NASA contract NAS5-26555), and by NASA grant NAG 5-3556. We thank Aaron Barth and Henrique Schmitt for helpful discussions on various aspects of this work. We are grateful to an anonymous referee for constructive comments.

TABLE 4  
SUPPLEMENTARY H $\alpha$  LUMINOSITIES

Galaxy	$\log(L_{\text{H}\alpha}/\text{erg s}^{-1})$	Galaxy	$\log(L_{\text{H}\alpha}/\text{erg s}^{-1})$
IC 239	36.89	NGC 4382	<38.10
IC 342	38.00	NGC 4388	40.26
NGC 147	<35.19	NGC 4406	<37.82
NGC 205	<34.79	NGC 4414	38.47
NGC 221	<36.19	NGC 4417	<37.88
NGC 507	<38.74	NGC 4421	<37.37
NGC 628	<36.69	NGC 4424	39.56
NGC 821	<38.13	NGC 4442	<37.98
NGC 1023	<37.82	NGC 4450	38.51
NGC 1052	39.45	NGC 4461	<37.92
NGC 1068	41.53	NGC 4473	<38.06
NGC 1358	40.19	NGC 4478	<37.67
NGC 1667	40.17	NGC 4494	<37.54
NGC 2300	<38.19	NGC 4503	<37.67
NGC 2403	39.86	NGC 4527	40.12
NGC 2549	<38.05	NGC 4564	<37.83
NGC 2634	<38.07	NGC 4569	40.28
NGC 2639	40.48	NGC 4570	<38.02
NGC 2768	38.78	NGC 4578	<37.58
NGC 2775	<37.94	NGC 4608	<37.65
NGC 2841	38.80	NGC 4612	<37.63
NGC 2911	39.38	NGC 4621	<37.99
NGC 2950	<38.42	NGC 4638	<37.93
NGC 2985	38.36	NGC 4648	<38.41
NGC 3034	41.20	NGC 4649	<37.73
NGC 3077	38.36	NGC 4665	<37.93
NGC 3115	<37.80	NGC 4736	37.81
NGC 3310	40.53	NGC 4754	<38.01
NGC 3368	38.91	NGC 4826	38.87
NGC 3384	<37.56	NGC 4914	<38.84
NGC 3395	39.62	NGC 5055	38.62
NGC 3516	39.99	NGC 5194	39.80
NGC 3610	<38.55	NGC 5195	38.67
NGC 3613	<38.32	NGC 5273	38.70
NGC 3640	<38.18	NGC 5473	<38.39
NGC 3642	39.38	NGC 5474	37.31
NGC 3838	<38.12	NGC 5523	39.06
NGC 3898	38.91	NGC 5548	40.22
NGC 3949	38.63	NGC 5576	<38.49
NGC 4026	<38.10	NGC 5585	37.69
NGC 4051	39.68	NGC 5676	39.04
NGC 4125	39.09	NGC 5701	38.22
NGC 4151	40.94	NGC 5746	39.25
NGC 4152	39.92	NGC 5775	39.53
NGC 4179	<38.45	NGC 5813	38.64
NGC 4251	<37.74	NGC 5850	39.25
NGC 4267	<37.88	NGC 5921	39.15
NGC 4291	<38.38	NGC 6654	<38.11
NGC 4339	<38.02	NGC 6946	39.96
NGC 4365	<37.98	NGC 7332	<38.03
NGC 4371	<37.61	NGC 7457	<37.24
NGC 4379	<37.63	...	...

## APPENDIX

SUPPLEMENTARY H $\alpha$  LUMINOSITIES FOR THE PALOMAR SURVEY

The catalog of H $\alpha$  luminosities presented in Paper III contains a number of entries that were not reliable because they were based on observations taken under nonphotometric conditions<sup>6</sup>. Table 4 gives an updated list of H $\alpha$  luminosities for those galaxies for which we were able to locate published H $\alpha$  fluxes. Most of the data come from the surveys by Heckman, Balick, & Crane (1980), Stauffer (1982a), and Keel (1983a). The luminosities are based on the distances given in Paper III, and they have been corrected for Galactic and internal extinction using the values of Galactic extinction and Balmer decrements given in Paper III. In addition to the literature data, Table 4 also includes ( $3\sigma$ ) upper limits for the H $\alpha$  luminosities of all absorption-line nuclei observed under photometric conditions. The luminosity upper limits were computed by combining the continuum flux density at 6600 Å with the  $3\sigma$  upper limits for the equivalent width of H $\alpha$  emission (see Paper III), assuming a line width of FWHM = 250 km s<sup>-1</sup>.

<sup>6</sup> In Paper III, we listed the nonphotometric measurements as lower limits. This is not strictly correct. Line fluxes measured under nonphotometric conditions can be either too high or too low compared to the true value; they are simply inaccurate.

## REFERENCES

- Alonso-Herrero, A., Rieke, M. J., Rieke, G. H., & Shields, J. C. 2000, *ApJ*, 530, 688
- Antonucci, R. R. J. 1993, *ARA&A*, 31, 473
- Antonucci, R. R. J., & Miller, J. S. 1985, *ApJ*, 297, 621
- Baldwin, J. A., Phillips, M. M., & Terlevich, R. 1981, *PASP*, 93, 5
- Balzano, V. A., & Weedman, D. W. 1981, *ApJ*, 243, 756
- Barnes, J. E., & Hernquist, L. E. 1991, *ApJ*, 370, L65
- Barth, A. J. 2002, in *Issues in Unification of AGNs*, ed. R. Maiolino, A. Marconi, & N. Nagar (San Francisco: ASP), 147
- Barth, A. J., Ho, L. C., Filippenko, A. V., Rix, H.-W., & Sargent, W. L. W. 2001, *ApJ*, 546, 205
- Barth, A. J., Ho, L. C., Filippenko, A. V., & Sargent, W. L. W. 1998, *ApJ*, 496, 133
- Barth, A. J., & Shields, J. C. 2000, *PASP*, 112, 753
- Bertola, F., Bettoni, D., Rusconi, L., & Sedmak, G. 1984, *AJ*, 89, 356
- Binette, L. 1985, *A&A*, 143, 334
- Cai, W., & Pradhan, A. K. 1993, *ApJS*, 88, 329
- Cardelli, J. A., Clayton, G. C., & Mathis, J. S. 1989, *ApJ*, 345, 245
- Combes, F. 2001, in *Advanced Lectures on the Starburst-AGN Connection*, ed. I. Aretxaga, D. Kunth, & R. Mújica (Singapore: World Scientific), 223
- Conti, P. S. 1991, *ApJ*, 377, 115
- Dahari, O., & De Robertis, M. M. 1988, *ApJS*, 67, 249
- De Robertis, M. M., & Osterbrock, D. E. 1984, *ApJ*, 286, 171
- . 1986, *ApJ*, 301, 727
- Dopita, M. A., Koratkar, A. P., Allen, M. G., Tsvetanov, Z. I., Ford, H. C., Bicknell, G. V., & Sutherland, R. S. 1997, *ApJ*, 490, 202
- Dopita, M. A., & Sutherland, R. S. 1995, *ApJ*, 455, 468
- Dressler, A. 1980, *ApJ*, 236, 351
- Efstathiou, A., & Rowan-Robinson, M. 1995, *MNRAS*, 273, 649
- Feigelson, E. D., & Babu, G. J. 1992, *ApJ*, 397, 55
- Feigelson, E. D., & Nelson, P. I. 1985, *ApJ*, 293, 192
- Feldman, F. R., Weedman, D. W., Balzano, V. A., & Ramsey, L. W. 1982, *ApJ*, 256, 427
- Ferland, G. J., & Netzer, H. 1983, *ApJ*, 264, 105
- Filippenko, A. V. 1985, *ApJ*, 289, 475
- . 1996, in *The Physics of LINERs in View of Recent Observations*, ed. M. Eracleous et al. (San Francisco: ASP), 17
- Filippenko, A. V., & Halpern, J. P. 1984, *ApJ*, 285, 458
- Filippenko, A. V., & Sargent, W. L. W. 1985, *ApJS*, 57, 503 (Paper I)
- . 1988, *ApJ*, 324, 134
- Filippenko, A. V., & Terlevich, R. 1992, *ApJ*, 397, L79
- Fosbury, R. A. E., Melbold, U., Goss, W. M., & Dopita, M. A. 1978, *MNRAS*, 183, 549
- Gebhardt, K., et al. 2002, *ApJ*, in press (astro-ph/0209483)
- Gonçalves, A. C., Véron-Cetty, M.-P., & Véron, P. 1999, *A&AS*, 135, 437
- Halpern, J. P., & Steiner, J. E. 1983, *ApJ*, 269, L37
- Heckman, T. M. 1980, *A&A*, 87, 152
- . 1995, *ApJ*, 446, 101
- Heckman, T. M., Balick, B., & Crane, P. C. 1980, *A&AS*, 40, 295
- Heckman, T. M., Miley, G. K., van Breugel, W. J. M., & Butcher, H. R. 1981, *ApJ*, 247, 403
- Ho, L. C. 1996, in *The Physics of LINERs in View of Recent Observations*, ed. M. Eracleous et al. (San Francisco: ASP), 103
- . 1999a, *Adv. Space Res.*, 23 (5-6), 813
- . 1999b, *ApJ*, 516, 672
- . 2002, in *IAU Colloq. 184, AGN Surveys*, ed. R. F. Green, E. Ye. Khachikian, & D. B. Sanders (San Francisco: ASP), in press (astro-ph/0110439)
- Ho, L. C., Filippenko, A. V., & Sargent, W. L. W. 1993a, *ApJ*, 417, 63
- . 1995, *ApJS*, 98, 477 (Paper II)
- . 1996, *ApJ*, 462, 183
- . 1997a, *ApJS*, 112, 315 (Paper III)
- . 1997b, *ApJ*, 487, 568 (Paper V)
- . 1997c, *ApJ*, 487, 579
- . 1997d, *ApJ*, 487, 591
- Ho, L. C., Filippenko, A. V., Sargent, W. L. W., & Peng, C. Y. 1997e, *ApJS*, 112, 391 (Paper IV)
- Ho, L. C., Rudnick, G., Rix, H.-W., Shields, J. C., McIntosh, D. H., Filippenko, A. V., Sargent, W. L. W., & Eracleous, M. 2000, *ApJ*, 541, 120
- Ho, L. C., Shields, J. C., & Filippenko, A. V. 1993b, *ApJ*, 410, 567
- Ho, L. C., & Ulvestad, J. S. 2001, *ApJS*, 133, 77
- Holmberg, E. 1975, in *Stars and Stellar Systems*, Vol. 9, *Galaxies and the Universe*, ed. A. Sandage, M. Sandage, & J. Kristian (Chicago: Univ. Chicago Press), 123
- Huchra, J. P., & Burg, R. 1992, *ApJ*, 393, 90
- Isobe, T., Feigelson, E. D., & Nelson, P. I. 1986, *ApJ*, 306, 490
- Keel, W. C. 1983a, *ApJS*, 52, 229
- . 1983b, *ApJ*, 268, 632
- . 1983c, *ApJ*, 269, 466
- Koski, A. T. 1978, *ApJ*, 223, 56
- Koski, A. T., & Osterbrock, D. E. 1976, *ApJ*, 203, L49
- Leitherer, C., et al. 1999, *ApJS*, 123, 3
- Magorrian, J., et al. 1998, *AJ*, 115, 2285
- Maoz, D., Barth, A. J., Ho, L. C., Sternberg, A., & Filippenko, A. V. 2001, *AJ*, 121, 3048
- Maoz, D., Filippenko, A. V., Ho, L. C., Rix, H.-W., Bahcall, J. N., Schneider, D. P., & Macchetto, F. D. 1995, *ApJ*, 440, 91
- Maoz, D., Koratkar, A. P., Shields, J. C., Ho, L. C., Filippenko, A. V., & Sternberg, A. 1998, *AJ*, 116, 55
- Mulchaey, J. S., Wilson, A. S., & Tsvetanov, Z. 1996, *ApJ*, 467, 197
- Nelson, C. H., & Whittle, M. 1996, *ApJ*, 465, 96
- Péquignot, D. 1984, *A&A*, 131, 159
- Phillips, M. M., Charles, P. A., & Baldwin, J. A. 1983, *ApJ*, 266, 485
- Phillips, M. M., Jenkins, C. R., Dopita, M. A., Sadler, E. M., & Binette, L. 1986, *AJ*, 91, 1062 (erratum: 1986, *AJ*, 92, 503)
- Pier, E. A., & Krolik, J. H. 1992, *ApJ*, 401, 99
- Pogge, R. W. 1989a, *ApJS*, 71, 433
- . 1989b, *ApJ*, 345, 730
- Pogge, R. W., Maoz, D., Ho, L. C., & Eracleous, M. 2000, *ApJ*, 532, 323
- Postman, M., & Geller, M. J. 1984, *ApJ*, 281, 95
- Press, W. H., Flannery, B. P., Teukolsky, S. A., & Vetterling, W. T. 1986, *Numerical Recipes: The Art of Scientific Computing* (Cambridge: Cambridge Univ. Press)
- Roberts, M. S., & Haynes, M. P. 1994, *ARA&A*, 32, 115
- Sabra, B. M., Shields, J. C., Ho, L. C., Barth, A. J., & Filippenko, A. V. 2002, *ApJ*, submitted
- Schaerer, D., & Vacca, W. D. 1998, *ApJ*, 497, 618
- Schmitt, H. R. 2001, *AJ*, 122, 2243
- Schmitt, H. R., Antonucci, R. R. J., Ulvestad, J. S., Kinney, A. L., Clarke, C. J., & Pringle, J. E. 2001, *ApJ*, 555, 663
- Shaw, R. A., & Dufour, R. J. 1995, *PASP*, 107, 896
- Shields, J. C. 1992, *ApJ*, 399, L27
- Shuder, J. M., & Osterbrock, D. E. 1981, *ApJ*, 250, 55
- Stasińska, G. 1984, *A&A*, 135, 341
- Stauffer, J. R. 1982a, *ApJS*, 50, 517
- . 1982b, *ApJ*, 262, 66
- Sugai, H., & Malkan, M. A. 2000, *ApJ*, 529, 219
- Taniuchi, Y., Shioya, Y., & Murayama, T. 2000, *AJ*, 120, 1265
- Terlevich, R., & Melnick, J. 1985, *MNRAS*, 213, 841
- Tully, R. B. 1988, *Nearby Galaxies Catalog* (Cambridge: Cambridge Univ. Press)
- Veilleux, S., & Osterbrock, D. E. 1987, *ApJS*, 63, 295
- Véron, P., Gonçalves, A. C., & Véron-Cetty, M.-P. 1997, *A&A*, 319, 52
- Véron, P., & Véron-Cetty, M.-P. 1986, *A&A*, 161, 145
- Weedman, D. W. 1970, *ApJ*, 159, 405
- . 1977, *ARA&A*, 15, 69
- Whitmore, B. C., Zhang, Q., Leitherer, C., Fall, S. M., Schweizer, F., & Miller, B. W. 1999, *AJ*, 118, 1551
- Whittle, M. 1985a, *MNRAS*, 213, 1
- . 1985b, *MNRAS*, 213, 33
- . 1985c, *MNRAS*, 216, 817
- . 1992, 387, 121
- . 1993, in *The Nearest Active Galaxies*, ed. J. Beckman, L. Colina, & H. Netzer (Madrid: CSIC Press), 63
- Wills, B. J. 1999, in *Quasars and Cosmology*, ed. G. Ferland & J. Baldwin (San Francisco: ASP), 101
- Wilson, A. S., & Heckman, T. M. 1985, in *Astrophysics of Active Galaxies and Quasi-Stellar Objects*, ed. J. S. Miller (Mill Valley, CA: Univ. Science Books), 39